



AD 748895

AD

RESEARCH AND DEVELOPMENT  
TECHNICAL REPORT ECOM-0129-F

A  
THEORETICAL AND EXPERIMENTAL  
INVESTIGATION OF PLANAR  
PIN THERMOPHOTOVOLTAIC  
CELLS

FINAL REPORT

By  
R. J. Schwartz  
N. F. Gardner

DDC  
RECEIVED  
SEP 27 1972  
B

AUGUST 1972

SEE AD 730771

ECOM

UNITED STATES ARMY ELECTRONICS COMMAND · FORT MONMOUTH, N.J.

CONTRACT DAAB07-70-C-0129  
SCHOOL OF ELECTRICAL ENGINEERING  
PURDUE UNIVERSITY  
WEST LAFAYETTE, INDIANA

DISTRIBUTION STATEMENT  
Approved for public release;  
distribution unlimited

Reproduced by  
NATIONAL TECHNICAL  
INFORMATION SERVICE  
U S Department of Commerce  
Springfield VA 22151

**Best  
Available  
Copy**

# NOTICES

## Disclaimers

The findings in this report are not to be construed as an official Department of the Army position, unless so designated by other authorized documents.

The citation of trade names and names of manufacturers in this report is not to be construed as official Government indorsement or approval of commercial products or services referenced herein.

## Disposition

Destroy this report when it is no longer needed. Do not return it to the originator.

ACCESSION for	
NTIS	White Section <input checked="" type="checkbox"/>
DSG	Ref: Section <input type="checkbox"/>
UNANNOUNCED	<input type="checkbox"/>
JUSTIFICATION .....	
BY .....	
DISTRIBUTION/AVAILABILITY CODES	
Dist.	AvAIL. and/or SPCLIAL
A	

## DOCUMENT CONTROL DATA - R &amp; D

(Security classification of title, body of abstract and indexing annotation must be entered when the overall report is classified)

1. ORIGINATING ACTIVITY (Corporate author) Purdue University Lafayette, Indiana 47907		2a. REPORT SECURITY CLASSIFICATION Unclassified	
		2b. GROUP	
3. REPORT TITLE A Theoretical and Experimental Investigation of Planar PIN Thermophotovoltaic Cells			
4. DESCRIPTIVE NOTES (Type of report and inclusive dates) Final Report (June 1970 - June 1972)			
5. AUTHOR(S) (First name, middle initial, last name) R. J. Schwartz and N. F. Gardner			
6. REPORT DATE August 1972	7a. TOTAL NO. OF PAGES 85	7b. NO. OF REFS	
8a. CONTRACT OR GRANT NO. DAAB07-70-C-0129	9a. ORIGINATOR'S REPORT NUMBER(S)		
b. PROJECT NO. ITO 61102 A 30 A			
c. Task No. -02	9b. OTHER REPORT NO(S) (Any other numbers that may be assigned this report) ECOM-0129- <del>6</del>		
d. Subtask No. -312			
10. DISTRIBUTION STATEMENT Approved for public release; distribution unlimited.			
11. SUPPLEMENTARY NOTES		12. SPONSORING MILITARY ACTIVITY US Army Electronics Command ATTN: AMSRL-TL-RE Fort Monmouth, N w Jersey 07703	
13. ABSTRACT The results of calculations of the performance of a planar p-i-n thermophotovoltaic cell are reported. A computer program has been written which automatically optimizes the cell geometry. The program allows the bulk recombination rate, the surface recombination velocity, the hole and electron mobilities and the intensity and spectrum of radiation illuminating the cell to be chosen arbitrarily. The performance of german p-i-n cells is investigated for monochromatic radiation and radiation from 1873°K erbium oxide and black body sources.  Experimental work leading to the fabrication of interdigitated p-i-n thermophotovoltaic cells is described. The results of tests evaluating the performance of fabricated cells are discussed. A series of experiments were carried out to determine why the performance of these cells was below theoretical expectations.  Details of illustrations in this document may be better studied on microfiche			

4 KEY WORDS	LINK A		LINK B		LINK C	
	ROLE	WT	ROLI	WT	ROLE	WT
Thermophotovoltaic Energy Conversion Photovoltaic Cell Germanium PIN-Junction Device						

TR ECOM-0129-F  
AUGUST 1972

REPORTS CONTROL SYMBOL  
OSD - 1366

A THEORETICAL AND EXPERIMENTAL  
INVESTIGATION OF PLANAR PIN  
THERMOPHOTOVOLTAIC CELLS

REPORT NO. 2  
JUNE 1970-JUNE 1972  
CONTRACT NO. DAAB07-70-C-0129  
DA PROJECT NO. ITO 61102 A36A-02-31

Prepared By  
R. J. Schwartz  
N. F. Gardner  
School of Electrical Engineering  
PURDUE UNIVERSITY  
West Lafayette, Ind.

For  
U.S. Army Electronics Command  
Fort Monmouth, N. J.

Distribution Statement  
Approved for public release;  
distribution unlimited

ABSTRACT

The results of calculations of the performance of a planar p-i-n thermophotovoltaic cell are reported. A computer program has been written which automatically optimizes the cell geometry. The program allows the bulk recombination rate, the surface recombination velocity, the hole and electron mobilities and the intensity and spectrum of radiation illuminating the cell to be chosen arbitrarily. The performance of germanium p-i-n cells is investigated for monochromatic radiation and radiation from 1873<sup>o</sup>K erbium oxide and black body sources.

Experimental work leading to the fabrication of interdigitated p-i-n thermophotovoltaic cells is described. The results of tests evaluating the performance of fabricated cells are discussed. A series of experiments were carried out to determine why the performance of these cells was below theoretical expectations.

CONTENTS

	<u>Page</u>
LIST OF SYMBOLS	-iv-
LIST OF TABLES	-v-
LIST OF FIGURES	-vi-
INTRODUCTION	1
I. THEORETICAL INVESTIGATIONS	4
A. Introduction	4
B. Lifetime Considerations	4
C. Results	6
1. Monochromatic radiation	6
2. Radiation from an erbium oxide source	15
3. Radiation from a black body Source	22
II. EXPERIMENTAL INVESTIGATIONS	24
A. Introduction	24
B. Description of Device Fabrication Process	24
C. Experimental Investigations of the Fabrication Process	26
1. Insulator deposition	26
Silicon dioxide deposition	26
Aluminum oxide deposition	27
Photoresist problems with silicon dioxide films	27
2. Contact formation	27
n contacts	28
Chemical etching	30
Ultrasonic etching	30
Photoresist liftoff etching	30
Arsenic doped contacts	31
p contacts	31
Alloying	32
Junction staining solution	32
Alloying technique	33
Aluminum films	33
Indium films	34
Aluminum on indium films	34
Antimony on gold films	34
Antimony films	35
Tin-Antimony-tin films	35
Conclusions	35
Contact buildup	36

	<u>Page</u>
3. Fabrication problems	37
Compatability of etchants and processing chemicals	37
Problems with gold contacting aluminum	37
4. Heat sink fabrication and device mounting	40
5. Evaluation of heat sink performance	41
D. Performance of Fabricated Devices	42
E. Investigation of Deficiencies in Devices	45
1. Contact Deficiencies	45
2. Lifetime damage due to silicon dioxide deposition	46
3. Determination of the dominant source of recombination	49
4. Conclusions	53
III. CONCLUSIONS AND RECOMMENDATIONS FOR FUTURE WORK	54
REFERENCES	56
APPENDIX	57
PRINTOUT OF ADOP PROGRAM	72

SYMBOL LIST\*

- $l_n$  = width of n contact
- $l_p$  = width of p contact
- $l_i$  = spacing between contacts
- $x_0$  = thickness of device
- $n$  = excess carrier concentration
- $e$  = electron charge
- $n_i$  = intrinsic carrier concentration
- $V$  = voltage
- $k$  = Boltzmann's constant
- $T$  = temperature in  $^{\circ}\text{K}$

---

\* All symbols used in the FORTRAN program are defined in Tables XII and XIII.

TABLES

	<u>Page</u>
I. Optimum Dimensions and Output Parameters of Devices Illuminated with Monochromatic Radiation	8
II. Dependence of Output Parameters on Device Thickness	10
III. Variation in Maximum Power Output for Different Contact Widths	13
IV. Optimum Dimensions and Output Parameters of Devices Illuminated with 1873 <sup>o</sup> K Erbium Oxide Spectrum	16
V. Optimum Dimensions and Output Parameters of Devices with Finite Bulk Lifetimes	20
VI. Optimum Dimensions and Output Parameters of Devices Illuminated with 1873 <sup>o</sup> K Black Body Spectrum	23
VII. Effects of Chemicals and Etchants on Metals and Insulators	38
VIII. Etchants Used in Device Fabrication	39
IX. Open Circuit Voltage Output of Fabricated Devices	43
X. Open Circuit Voltage Output of Dot Pattern Devices	47
XI. Effect of Silicon Dioxide Deposition on Excess Carrier Concentration	51
XII. Relative Conductivity as a Function of Surface Bias	52
XIII. List of Physical Parameters	61
XIV. List of Output Parameters	64
XV. Printed Output for a Given Set of Dimensions	67
XVI. Summary of Outputs for Given Sets of Dimensions and Output for Optimized Device	68

FIGURE LIST

	<u>Page</u>
FIGURE 1 Planar p-i-n Thermophotovoltaic Cell	2
FIGURE 2 Excess Carrier Concentration and Open Circuit Voltage at Which Bulk Radiative Recombination Equals Bulk Trap Recombination	5
FIGURE 3 Performance Characteristics for Cells Optimized for Monochromatic Radiation	11
FIGURE 4 Current-Voltage Curves of Devices Illuminated with Erbium Oxide Spectrum	17
FIGURE 5 Performance Characteristics of Cell Optimized for Radiation from an Erbium Oxide Source	19
FIGURE 6 Current - Voltage Curves of Devices with Finite Bulk Lifetimes	21
FIGURE 7 Partially Fabricated p-i-n Thermophotovoltaic Cell	25
FIGURE 8 Completely Fabricated p-i-n Thermophotovoltaic Cell	25
FIGURE 9 p-i-n Cell Mounted in Water Cooled Heat Sink	41
FIGURE 10 Current-Voltage Curve for Device #6	44
FIGURE 11 Current-Voltage Curve for Device #6 with Reverse Bias Applied	44
FIGURE 12 Sample Used to Test Effect of Silicon Dioxide Deposition on Lifetime.	48
FIGURE 13 Apparatus Used to Test Effect of Silicon Dioxide Deposition on Lifetime	50

## INTRODUCTION

This is a final report on the work which was performed under contract number DAAB07-70-C-0129. This report contains a detailed description of the work performed from June 1, 1971 to June 1, 1972 under the above contract. Previous work covering the period from June 1, 1970 to June 1, 1971 which was performed under the same contract has been reported in the annual report TR ECOM-0129-1. This report, which will be referred to as Report No. 1,<sup>1</sup> was published in August, 1971 with the control symbol OSD-1366.

The purposes of this contract were to theoretically investigate germanium p-i-n planar photovoltaic cells, to determine the optimum design of such cells for thermophotovoltaic use and to fabricate germanium p-i-n cells which represent the present state of the art. Figure 1 shows a cross section view and a view from the contact side of a planar p-i-n structure.

One of the purposes of this investigation is to determine if the p-i-n structure has a significant advantage over the standard p-n photovoltaic cell in thermophotovoltaic applications. In order to do this, the performance of the p-i-n cell had to be analyzed under a variety of operating conditions. This was done with a computer program which would allow the computation of cell performance under a variety of specified incident radiation spectra as well as a variety of materials parameters such as surface recombination velocity, bulk recombination rate and mobility. The computer program was described in Report No. 1.<sup>1</sup> During the last year of the contract this program has been expanded to allow for automatic optimization of the device dimensions when the incident radiation spectrum,

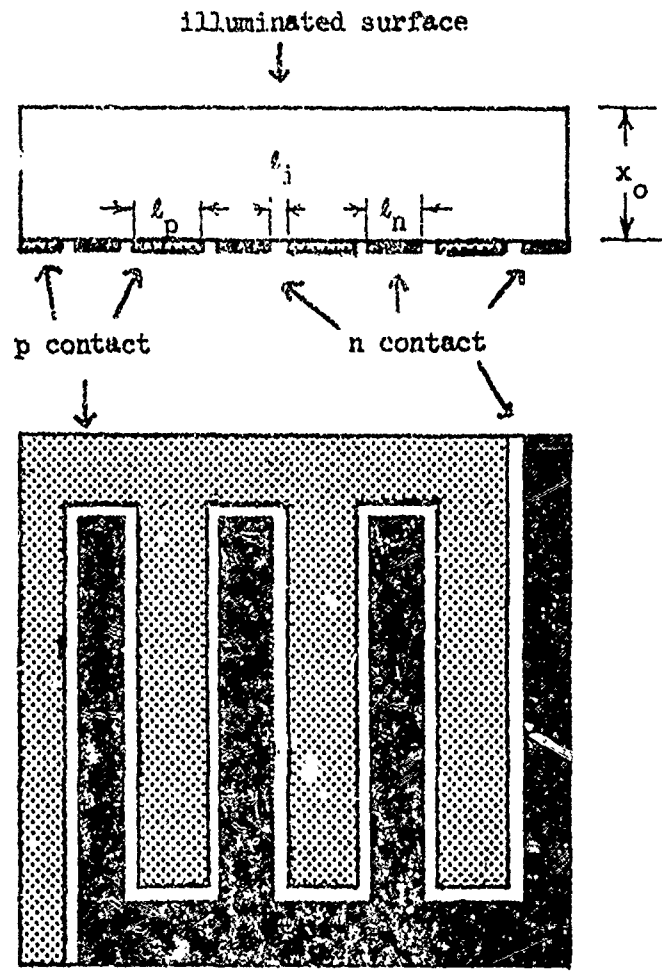


Figure 1. Planar p-i-n Thermophotovoltaic Cell

surface recombination velocity and the bulk recombination rate are specified. The first part of this report deals with the results of this optimization program.

Three distinct types of radiation spectra were selected for study - monochromatic radiation, black body radiation at  $1873^{\circ}\text{K}$  and radiation from an erbium oxide radiator at  $1873^{\circ}\text{K}$ . The analysis with monochromatic radiation is of little practical value, but it provides insight into the performance of the cell with other radiation spectra. The analysis with the erbium oxide radiator is of interest, because the spectral emissivity of erbium oxide is relatively large for photons with energies near the direct gap in germanium and relatively small for photons with energies well above or well below the direct gap energy. Thus, radiation from an erbium oxide source can be converted into electrical energy more efficiently than radiation from a black body source.

The second part of this report deals with the experimental program. It contains a description of the procedure used to fabricate p-i-n photovoltaic cells and of the investigations that were carried out in connection with the fabrication process. The results which have been obtained to date on the performance of germanium p-i-n photovoltaic cells are discussed. A series of tests was carried out to determine why the performance of these cells is below theoretical expectations.

In the third part of the report the most significant theoretical and experimental results are briefly discussed and recommendations are made for future work.

## I. THEORETICAL INVESTIGATIONS

### A. Introduction

In Report No. 1<sup>1</sup> the results of the program to optimize the design for a device illuminated by black body radiation were described. It was clear from these results that additional optimization calculations needed to be performed to determine the effects of various spectra as well as the effects of changes in surface recombination velocity and bulk recombination rate on the performance of the device. A new program was written which utilized essentially the same approach for evaluating the performance of the device as the program described in Report No. 1<sup>1</sup> but which also automatically optimized the dimensions of the device. This Automatic Device Optimization Program (ADOP) is described in the appendix.

### B. Lifetime Considerations

In Report No. 1 we pointed out that in the usual operating range for a p-i-n photovoltaic cell, the lifetime of the excess carriers will be determined primarily by radiative recombination rather than by recombination through trap sites. In Figure 2 we show a curve of the excess carrier concentration as a function of minority carrier lifetime for which the rate of recombination due to recombination through trap sites is equal to the rate of recombination due to radiative recombination. The curve is also plotted in terms of open circuit voltage which can be correlated directly to excess carrier concentration. If the open circuit voltage for a particular minority carrier lifetime lies above the curve, the dominant recombination mechanism will be radiative

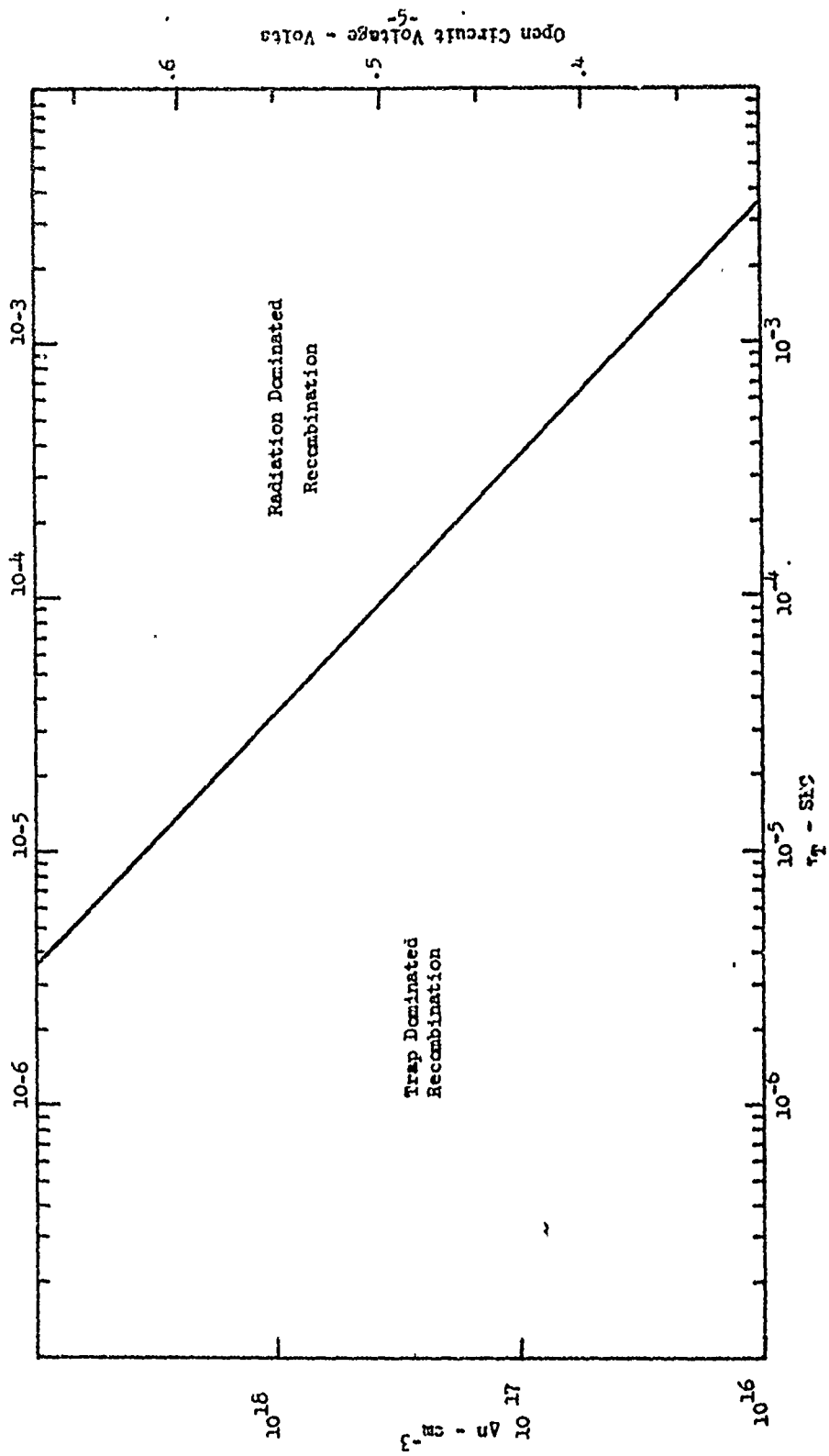


Figure 2. Excess Carrier Concentration and Open Circuit Voltage at Which Bulk Radiative Recombination Equals Bulk Trap Recombination

recombination. If the open circuit voltage lies below the curve, the dominant recombination mechanism will be recombination through trap sites. Since the minority carrier lifetime for the starting material is in excess of  $2 \times 10^{-3}$  seconds, it appears that for operating conditions which would normally be found in the operation of a photovoltaic cell, ( $\Delta N \approx 10^{17}$  electrons  $\text{cm}^{-3}$ ) the dominant recombination mechanism would be radiative recombination. If, however, the minority carrier lifetime in the bulk is significantly reduced during processing (say to a value of 10 to 100  $\mu$  sec.), then the dominant recombination mechanism would not be radiative recombination, and one should base lifetime calculations on the usual Hall-Shockley-Reed type recombination statistics. Since the purpose of using intrinsic material is to obtain a very high minority carrier lifetime in the bulk, we have assumed for all of our calculations that the dominant recombination mechanism is radiative recombination. The radiative recombination parameter is found to be equal to  $2.8 \times 10^{-17}$   $\text{cm}^3 \text{sec}^{-1}$  from fundamental thermodynamic arguments.<sup>6</sup> None of the devices, which are described in chapter II, were operated in the radiation recombination region during performance tests, performed under this contract. The reasons for this are discussed in chapters II and III.

#### C. Results

The results obtained from the ADOL program are summarized in Tables I, IV, V and VI. The results for monochromatic radiation will be analyzed in considerable detail. Many of the conclusions drawn from these results will be applicable to those obtained for black body radiation and radiation from an erbium oxide source.

##### 1. Monochromatic radiation.

The performance of the p-i-n cell has been analyzed for three different wavelengths of monochromatic radiation. The wavelengths were chosen so that their absorption lengths would vary over a range of values which would be

approximately equal to realistic values of device thickness ( $x_0$ ). The three wavelengths chosen were  $1.50 \mu\text{m}$ ,  $1.54 \mu\text{m}$  and  $1.60 \mu\text{m}$  with respective absorption lengths of  $2.3 \mu\text{m}$ ,  $21 \mu\text{m}$  and  $104 \mu\text{m}$ . An absorption length is defined as the distance into the germanium at which 63% of the incident radiation has been absorbed.

The results of the output obtained from the ADOP program for monochromatic radiation are summarized in Table I, and Figure 3. The spacing between contacts (LI) is fixed at  $25 \mu\text{m}$ . The maximum current collectable per unit area of illuminated surface, if every photon capable of generating a hole-electron is absorbed (CHROPT), is fixed at  $5 \text{ amps/cm}^2$ . The following observations can be made from the results in Table I:

- 1) When the excess carrier concentration is very large, the optimum device thickness is determined primarily by two conflicting factors. The device should be as thick as possible in order to absorb as much of the incident radiation as possible. On the other hand, as the device gets thicker the volume in which recombination can take place increases, while the relative increase in the number of photons absorbed tends to become smaller. Therefore the excess carrier concentration must decrease. This, of course, results in a reduction of output voltage.

The dependence of open circuit voltage and short circuit current on device thickness is shown in Table II. The data in this Table is obtained from the output of the program from which device 11 was optimized. Note that as  $X_0$  increases, the open circuit voltage and maximum power point voltages decrease, while the short circuit current and maximum power point current increase.

In cases where VSB and VST are both 0 (devices #1, 11 and 20), the optimum thickness ( $X_0$ ) is roughly four absorption lengths. About 90% of the incident photons are absorbed in four absorption lengths.

TABLE I

Optimum Dimensions and Output Parameters of Devices Illuminated with Monochromatic Radiation\*

Device	VSB (cm sec <sup>-1</sup> )	VST (cm sec <sup>-1</sup> )	L <sub>1</sub> (μm)	L <sub>2</sub> (μm)	L <sub>3</sub> (μm)	L <sub>4</sub> (μm)	X <sub>0</sub> (μm)	PMAKPOW (watt cm <sup>-2</sup> )	ETACELL (%)	ETACOL	ETAABS	g	VOC (Volts)	CURDSC (amp cm <sup>-2</sup> )
1	0	0	12.18	20.29	20.98	20.98	20.98	2.224	67.80	1.000	.9938	.8150	.5491	4.969
2	0	0	30.62	50.96	50.96	50.96	50+	2.049	82.10	1.000	1.000	.8036	.5100	5.000
3	10	10	118.7	200.9	200.9	200.9	50+	1.963	59.47	.999	1.000	.7772	.5056	4.95
4	100	100	130.5	224.4	224.4	224.4	50+	1.594	48.29	.9893	1.000	.6854	.4701	4.946
5	1000	1000	89.26	146.1	146.1	146.1	50+	.9551	28.94	.9036	1.000	.5861	.3607	4.518
6	0	10	30.67	51.14	51.14	51.14	50+	1.976	59.89	.9991	1.000	.7317	.5061	4.995
7	0	100	30.76	51.74	51.74	51.74	50+	1.634	49.50	.9909	1.000	.6958	.4739	4.954
8	0	1000	31.31	55.25	55.25	55.25	50+	1.027	31.13	.9164	1.000	.6073	.3692	4.582
9	10	0	131.9	224.7	224.7	224.7	50+	2.034	61.65	.5099	1.000	.7986	.5095	5.000
10	100	0	332.5	523.0	523.0	523.0	50+	1.966	60.17	Unreliable	1.000	.7463	.5078	Unreliable
11	0	0	56.25	83.57	83.57	83.57	91.83	1.942	59.65	.9999	.9864	.7971	.4939	4.932
12	10	10	123.0	203.7	203.7	203.7	99.33	1.879	57.45	.9966	.9910	.7769	.4888	4.948
13	100	100	169.0	282.3	282.3	282.3	114.5	1.570	47.79	.9840	.9954	.6950	.4612	4.987
14	1000	1000	136.4	210.4	210.4	210.4	94.83	.9569	29.29	.8637	.9900	.6012	.3638	4.375
15	0	10	56.19	83.72	83.72	83.72	96.47	1.886	57.76	.9986	.9906	.7801	.4894	4.946
16	0	100	56.27	84.36	84.36	84.36	111.6	1.601	48.72	.9849	.9958	.7039	.4639	4.904
17	0	1000	56.82	87.58	87.58	87.58	84.85	.9959	30.64	.9027	.9848	.6056	.3700	4.445
18	10	0	132.3	219.2	219.2	219.2	93.05	1.931	59.28	.9999	.9872	.7934	.4932	4.936
19	100	0	321.1	522.0	522.0	522.0	97.43	1.896	58.03	Unreliable	.9900	.7793	.4909	4.956

(Continued on next page)

\* Absorption Length = 1.50 μm

\* Absorption Length = 1.54 μm

(Table I continued)

Device #	VS <sub>B</sub> (cm sec <sup>-1</sup> )	VS <sub>T</sub> (cm sec <sup>-1</sup> )	LE (μ)	LP (μ)	XO (μ)	PMAXPOW (watt cm <sup>-2</sup> )	ETACELL (%)	ETA <sub>COL</sub>	ETA <sub>AB</sub>	GR	VOC (Volts)	CURDSC (amp cm <sup>-2</sup> )
20	0	0	128.1	197.2	376.0	1.694	52.81	.9969	.9722	.7658	.4565	4.846
21	10	10	154.6	236.9	361.7	1.661	51.69	.9922	.9738	.7563	.4546	4.831
22	100	100	215.7	350.4	390.6	1.437	44.59	.9534	.9762	.7004	.4407	4.654
23	1000	1000	216.1	360.5	297.0	.7865	25.30	.7754	.9420	.5868	.3670	3.652
24	0	10	119.7	187.0	360.6	1.664	51.60	.9923	.9736	.7575	.4584	4.830
25	0	100	126.6	197.0	363.7	1.452	45.01	.9533	.9756	.7064	.4420	4.651
26	0	1000	146.0	226.6	297.7	.8139	26.17	.7742	.9424	.6000	.3718	3.648
27	10	0	156.3	238.9	377.2	1.691	52.69	.9968	.9724	.7646	.4563	4.847
28	100	0	276.8	460.9	360.9	1.672	52.06	.9964	.9736	.7574	.4533	4.650

\* The FORTRAN variables given in this table are defined on pages in Table XIV. The estimated error in values of PMAXPOW is 1% or less. The values in the Table are listed as they appeared in the computer program printout. Although the output values are generally inaccurate beyond the second decimal place, small differences between two corresponding output values for different values of input parameters will generally be accurate to the third or fourth decimal place.

† Devices #1 through #10 are optimized under the constraint that the minimum attainable device thickness is 50 μm, because of limitations in fabrication technology.

WaveLength = 1.60 μm  
Absorption Length = 1.0 μm

TABLE II

Dependence of Output Parameters on Device Thickness \*

$\lambda = 1.54 \mu\text{m}$   
 $LN = 50 \mu\text{m}$      $LP = 75 \mu\text{m}$      $V_{SB} = V_{ST} = 0$

XO ( $\mu\text{m}$ )	VOC (volts)	CURDSC (amp $\text{cm}^{-2}$ )	VMAXPOW (volts)	CMAXPOW (amp $\text{cm}^{-2}$ )	PMAXPOW (watt $\text{cm}^{-2}$ )
25.0	.5186	3.475	.4441	3.274	1.454
37.5	.5127	4.158	.4385	3.913	1.716
50.0	.5075	4.535	.4334	4.263	1.848
62.5	.5029	4.743	.4289	4.455	1.911
75.0	.4988	4.858	.4249	4.558	1.937
87.5	.4951	4.921	.4213	4.614	1.944
100	.4918	4.956	.4181	4.642	1.941
125	.4861	4.986	.4124	4.661	1.922
150	.4814	4.995	.4077	4.661	1.900
175	.4773	4.997	.4035	4.656	1.879
200	.4738	4.996	.3999	4.648	1.859

\* The FORTRAN variables given in this table are defined in Table XIV. The data is obtained from the output of the program from which device 11 of Table I was optimized.



2) In cases where  $V_{ST}$  and  $V_{SB}$  are both 0 (device #1, 11 and 20),  $P_{MAXPOW}$  increases as the absorption length decreases. This is because the optimum value of  $X_0$  is smaller and therefore the volume in which excess carriers are generated is smaller. Hence, the number of carriers generated per unit volume is greater, and the open circuit voltage developed at the contacts is greater. This conclusion can be corroborated by a comparison of open circuit voltages for devices 1, 11 and 20. Note that the relative variation in open circuit voltage is much greater than the relative variation in short circuit current.

A second advantage resulting from larger excess carrier concentrations is a reduction in the resistivity of the bulk and, therefore, a reduction in ohmic loss due to the flow of current between contacts. However, this effect is almost negligible for the large excess carrier concentrations in devices 1, 11 and 20.

3) It would appear that the optimum contact widths  $L_N$  and  $L_P$  exhibit a strong dependence on the surface recombination velocity. For instance, in the case of devices 2 and 3, a small increase in the values of  $V_{SB}$  and  $V_{ST}$  from 0 to  $10 \text{ cm sec}^{-1}$  causes the optimum value of  $L_N$  to change from  $31 \mu\text{m}$  to  $119 \mu\text{m}$  and the optimum value of  $L_P$  to change from  $51 \mu\text{m}$  to  $201 \mu\text{m}$ . These changes, however, are not significant; for even though the optimum contact sizes change greatly, the output power is quite independent of contact sizes for small values of surface recombination velocity. This is shown for devices 2 and 3 in Table III. These devices are illuminated with radiation of a  $1.50 \mu\text{m}$  wavelength. The output power shows similar lack of dependence on  $L_N$  and  $L_P$  for samples illuminated with radiation of other wavelengths when surface recombination velocities are small.

TABLE III

Variation in Maximum Power Output for Different Contact Widths  
(Devices 2 and 3 from Table I)

$X_0 = 50 \mu\text{m}$

VBS ( $\text{cm sec}^{-1}$ )	VST ( $\text{cm sec}^{-1}$ )	LN ( $\mu\text{m}$ )	LP ( $\mu\text{m}$ )	P <sub>MAXPOW</sub> ( $\text{watt cm}^{-2}$ )
0	0	30.6*	51.0*	2.049
		5	100	2.048
		25	100	2.048
		12.5	50	2.048
		25	37.5	2.049
10	10	118.7*	200.9*	1.963
		150	250	1.962
		150	250	1.960
		50	200	1.961
		150	150	1.962

\*Optimized dimensions.

4) As VSB increases while VST is held constant at 0 (devices 9, 10, 18, 19, 27 and 28), there is a tendency for LN and LP to increase. The effect of increasing LN and LP while holding LI constant is to decrease the fraction of the unilluminated surface which is subject to surface recombination. Thus, fewer excess carriers are lost due to recombination on the unilluminated surface. This tendency for the contact size to increase is counterbalanced by an increase in the series resistance in the device as the average distance between the center of the p contact and the center of the n contact is increased. Thus, as the recombination velocity on the rear surface increases from a value of zero to a larger value, we observe LN and LP increasing until the series resistance begins to dominate.

5) In cases where VST is increases while VSB is held at 0 (devices 15-17 and 24-26) there is a tendency for the device thickness to increase slightly until VST exceeds 100 cm/sec. The tendency for the optimum device thickness to increase can be accounted for by realizing that as the surface recombination velocity increases the relative importance of bulk recombination velocity decreases. As  $X_0$  increases, the average excess carrier density decreases. This in turn, decreases the total recombination. Increasing  $X_0$  also increases the number of carriers generated, although the effect is quite small when  $X_0$  is greater than three absorption lengths. As the excess carrier concentration decreases, VOC decreases. Thus, the optimum value of  $X_0$  represents the best compromise between these competing needs. The optimum value of  $X_0$  will change as the relative importance of the surface recombination changes.

When the surface recombination velocity exceeds  $100 \text{ cm sec}^{-1}$ , the optimum thickness tends to decrease. This is because the excess carrier concentration becomes low enough to invalidate the assumption that the

excess carrier distribution is fairly uniform in the bulk region. Since most of the excess carriers are generated within one absorption length of the illuminated surface and since these carriers must diffuse to the contacts to be collected, the excess carrier concentration in the region of the contacts tends to be significantly less than the average excess carrier concentration in the bulk region when there is an appreciable current flowing through the contacts. Thus the maximum power point voltage will tend to be significantly reduced. The device tends to become thinner to minimize the reduction of excess carrier concentration in the region of the contacts due to the diffusion gradient.

6) In cases where VST and VSB are held equal (devices 2-5, 11-14 and 20-23), the effects of surface recombination occurring on the illuminated surface only and on the unilluminated surface only are combined. Thus,  $I_N$  and LP increase as VSB increases to  $100 \text{ cm sec}^{-1}$ , and (for devices 11-14 and 20-23)  $X_0$  increases as VST increases to 100, but starts to decrease as VST increases to 1000.

## 2. Radiation from an erbium oxide source

The results obtained from the ADOP program for devices illuminated with radiation from an  $1873^\circ\text{K}$  erbium oxide source are summarized in Tables IV and V. The current-voltage curves of these devices are plotted in Figures 4 and 6. In general the observations made for devices illuminated with monochromatic radiation are applicable to these devices.

For an idealized device (device 29) the conversion efficiency is 14.7%. If VST is held at 0, very little degradation of output power occurs for values of VSB smaller than  $100 \text{ cm sec}^{-1}$ . On the other hand, if VSB is held at 0, there is a significant degradation in the output power

TABLE IV  
Optimum Dimensions and Output Parameters of Devices Illuminated with 1873 Å Erbium Oxide Spectrum\*

Device	VSB (cm sec <sup>-1</sup> )	VSB (cm sec <sup>-1</sup> )	VSB (cm sec <sup>-1</sup> )	E <sub>1</sub> (eV)	E <sub>2</sub> (eV)	E <sub>3</sub> (eV)	E <sub>4</sub> (eV)	E <sub>5</sub> (eV)	PMAJOM (watt cm <sup>-2</sup> )	ETACELL (%)	ETAOL (%)	ETAABS	Q <sub>1</sub>	VOC (Volts)	CURDSC (amp cm <sup>-2</sup> )
Incident Power = 9.2 watt cm <sup>-2</sup>	0	0	0	128.5	196.8	401.2	1.350	51.79	.9966	.7894	.7634	.4493	3.936		
	10	10	10	155.6	239.3	417.8	1.320	50.42	.9903	.7936	.7525	.4466	3.929		
	100	100	100	218.6	356.8	437.0	1.122	42.62	.9387	.7576	.6946	.4314	3.743		
	500	500	500	207.1	341.5	266.6	.7466	30.03	.8425	.7534	.6125	.3841	3.174		
CURDOPT = 5 amp cm <sup>-2</sup>	1000	1000	1000	147.0	244.5	159.2	.5731	24.58	.8092	.7066	.5794	.3460	2.859		
	0	0	0	121.1	179.5	414.2	1.324	50.59	.9905	.7928	.7542	.4470	3.926		
	100	100	1000	125.2	196.2	453.2	1.134	43.13	.9386	.7968	.7007	.4328	3.740		
	0	0	0	108.9	162.0	160.7	0.5989	25.65	.8128	.7074	.5910	.3524			
	0	0	0	157.9	243.0	404.4	1.347	51.64	.9964	.7905	.7618	.4489	3.939		
	100	100	1000	293.9	465.8	414.1	1.33	50.92	.9959	.7928	.7540	.4476	3.947		
Incident Power = 16.4 watt cm <sup>-2</sup>	0	0	0	120.5	179.4	344.4	2.793	54.47	.9957	.7768	.7672	.4706	7.735		
	10	10	10	151.1	228.7	353.7	2.742	53.35	.9904	.7786	.7584	.4688	7.711		
	100	100	100	202.4	324.5	374.4	2.401	44.42	.9453	.7837	.7102	.4564	7.409		
	500	500	500	187.3	311.5	248.1	1.676	34.00	.8505	.7471	.6329	.4169	6.394		
CURDOPT = 10 amp cm <sup>-2</sup>	1000	1000	1000	152.5	252.8	159.6	1.311	28.10	.8116	.7069	.5986	.3817	5.737		
Incident Power = 1.84 watt cm <sup>-2</sup>	0	0	0	164.2	254.9	518.7	.2457	45.82	.9984	.8734	.7537	.4018	.8111		
	10	10	10	225.7	355.8	580.1	.2358	43.51	.9896	.8212	.7323	.3962	.8128		
	100	100	100	314.9	512.0	607.6	.1819	33.40	.9200	.8251	.6470	.3704	.7590		
	500	500	500	219.4	363.7	287.4	.1078	21.48	.8303	.7605	.5613	.3040	.6318		
CURDOPT = 1 amp cm <sup>-2</sup>	1000	1000	1000	159.6	264.1	169.9	.07839	16.67	.7929	.7125	.5254	.2641	.5649		

\* The FORTRAN variables given in this table are defined in Table XIV. The estimated error in values of PMAJOM is 1% or less. The values in the table are listed as they appeared in the computer program printout. Although the output values are generally inaccurate beyond the second decimal place, small differences between two corresponding output values for different values of input parameters will generally be accurate to the third or fourth decimal place.

Current Voltage Curves of Devices Illuminated with Erbium Oxide Spectrum.  
(Devices are labeled according to device numbers in Table IV.)

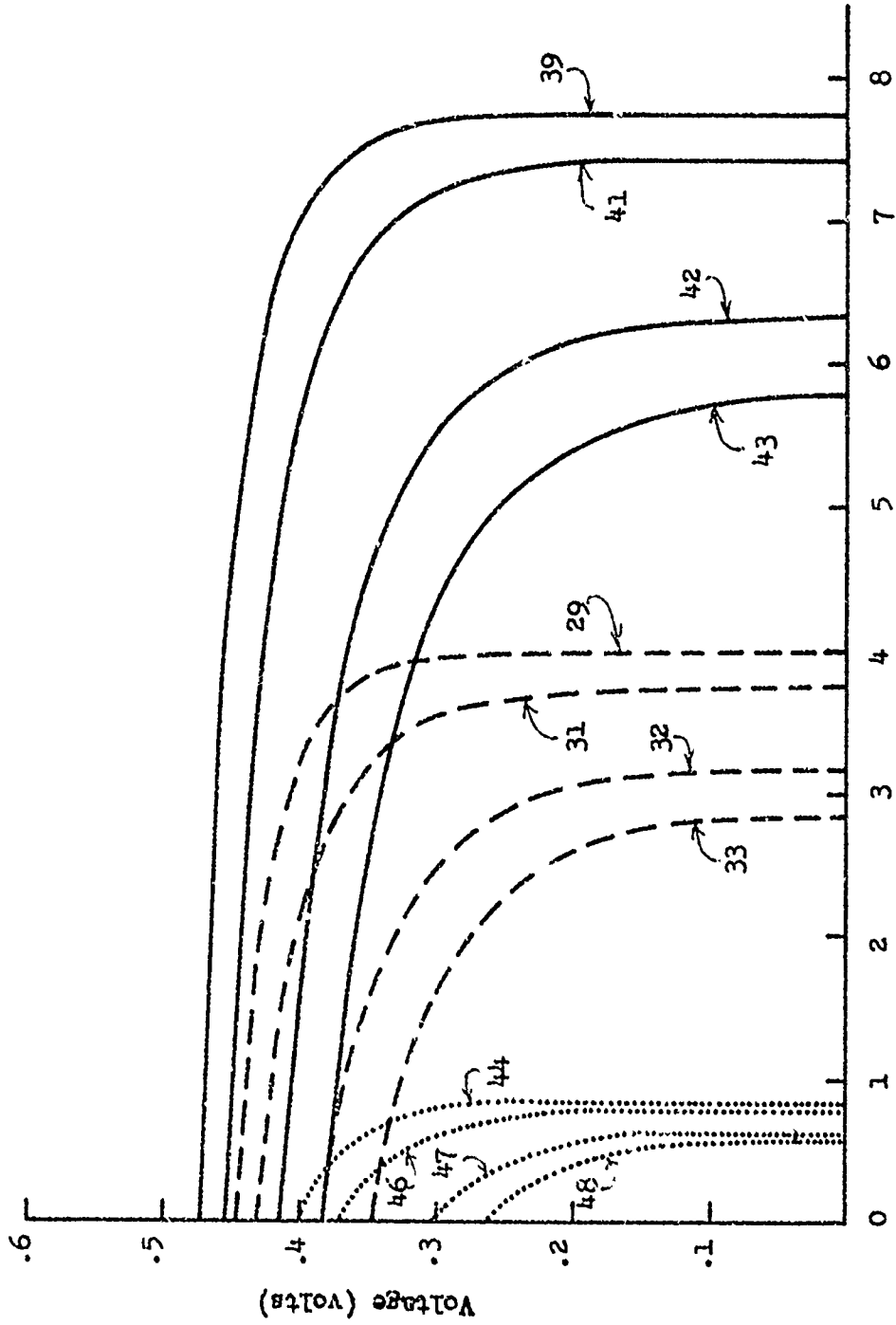


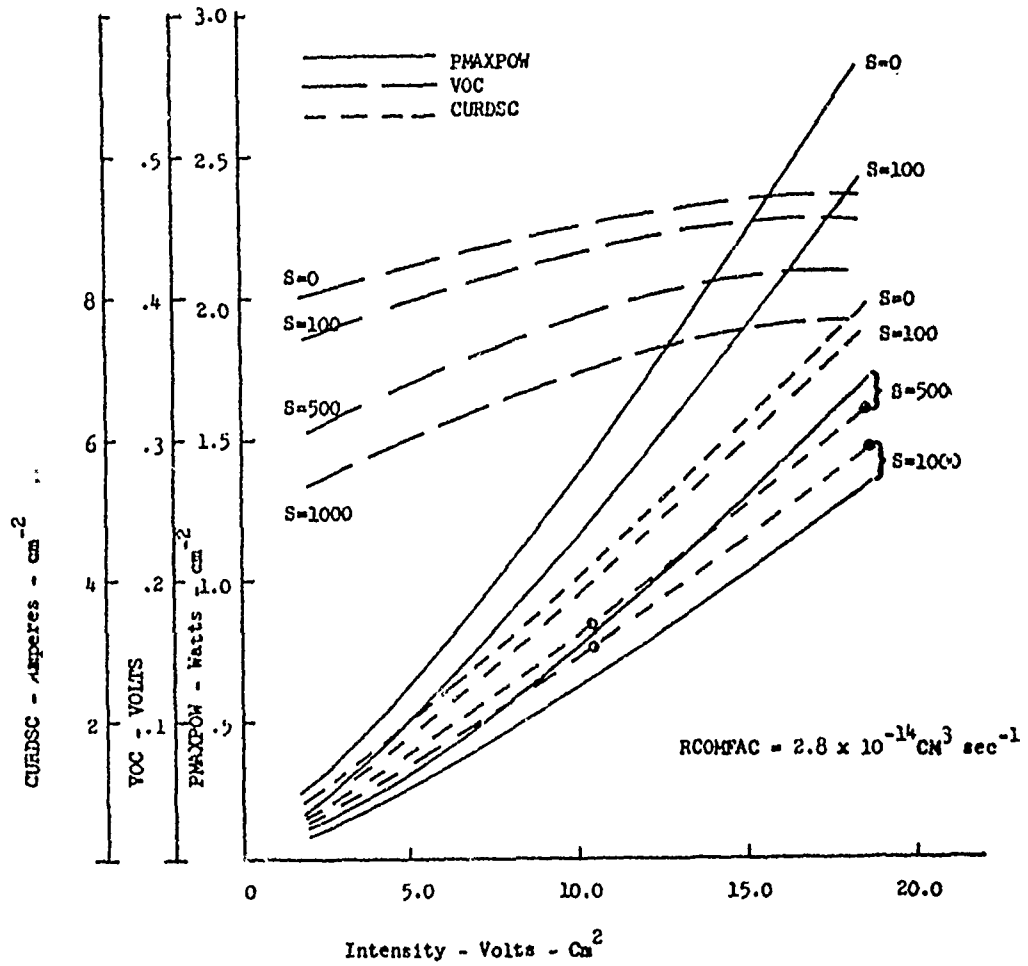
Figure 4. Current (AMPERES-CM<sup>-2</sup>)

as VST is increased from 0 to 100 cm sec<sup>-1</sup>. This is because the area of the illuminated surface is much greater than the area of the portion of the unilluminated surface between contacts.

For devices where the surface recombination velocity is the same on both the illuminated and unilluminated surfaces, the majority of the surface recombinations occur on the illuminated surface. However, it is expected that during processing it will be more difficult to maintain low surface recombination velocity on the unilluminated surface. Therefore, the total number of recombinations on either surface should be of comparable magnitude.

Some of the results of Table IV have been plotted in Figure 5. As would be expected the output power increases faster than a linear rate with increasing incident radiation intensity. However, because the radiative recombination increases as the square of the excess carrier concentration, the rate of rise in output power with increasing intensity is not as rapid as would be the case if all recombination occurred through trap sites.

The effect of recombination through trap sites is shown by the results summarized in Table V. These results are plotted in Figure 6. It is interesting to note that the open circuit voltages of devices 49 and 50 are greater than the open circuit voltage of device 29. This is because the recombination rate tends to vary linearly with the excess carrier concentration ( $n/\tau$ ) rather than with the square of the excess carrier concentration ( $rn^2$ ). Therefore, as the device becomes thinner, the relative increase in excess carrier concentration and open circuit voltage will be greater.



Performance characteristics of cells optimized for radiation from an Er<sub>2</sub>O<sub>3</sub> radiator. VSB-VST. See Table IV for device dimensions.

FIGURE 5

TABLE V

Optimum Dimensions and Output

Parameters of Devices with Finite Bulk Lifetimes\*

VSB = VST = 0    LI = 25 μM    RCOMFAC = 2.8 x 10<sup>.4</sup> cm<sup>3</sup> sec<sup>-1</sup>

Incident Power = 9.2 watt cm<sup>-2</sup>    CURDOPT = 5amp. cm<sup>-2</sup>

Device #	TAU (μ - sec)	LN (μM)	LP (μM)	XO (μM)	P/AXPOW (watt-cm <sup>-2</sup> )	ETACELL (%)	CF	VOC (volts)	CURDSC (amp-cm <sup>-2</sup> )
29	∞	128.5	196.8	401.2	1.350	51.79	.763 <sup>4</sup>	.4493	3.936
49	1000	116.0	169.3	289.3	1.272	50.66	.7461	.4517	3.774
50	100	54.95	81.71	78.70	1.024	48.08	.6973	.4578	3.207
51	10	31.03	53.48	50 <sup>+</sup>	.6975	34.74	.6210	.3778	2.966

\* The FORTRAN variables given in this Table are defined in Table XIV. The devices are illuminated with on 1873 Å Erbium Oxide Spectrum. The estimated error in [etc. (same as in Table IV.)]  
 +Device 51 is optimized under the constraint that the minimum attainable device thickness is 50 μM because of limitations in fabrication technology.

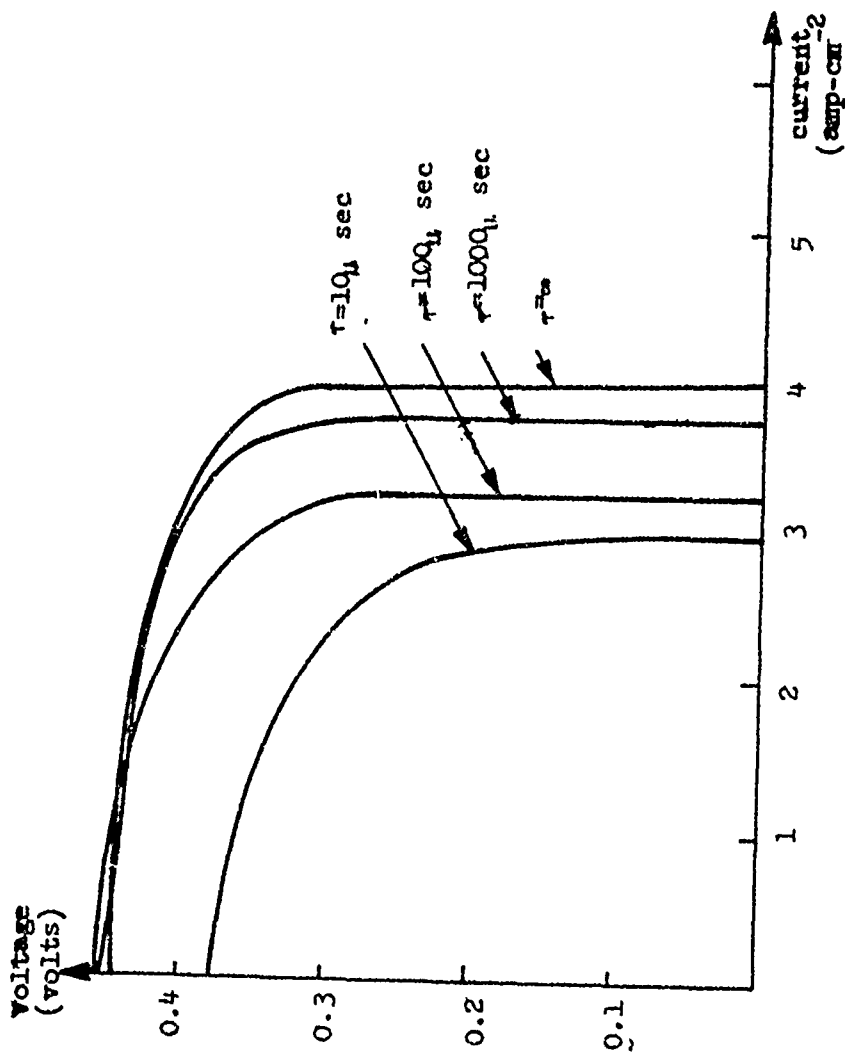


Figure 6. Current Voltage Curves of Devices with Finite Bulk Lifetimes

Consequently, the optimum thickness will tend to be smaller and the open circuit voltage will tend to be greater.

3. Radiation from a black body source

The results obtained from the ADOP program for devices illuminated with radiation from an 1873°K black body are summarized in Table V $\bar{I}$ . In general, for the same value of CURD $\bar{M}$ A $\bar{X}$ , the optimum device dimensions occurred at slightly larger values for black body radiation than for erbium oxide radiation. The conversion efficiency is also lower because a larger portion of the radiation energy is in unfavorable portions of the energy spectrum. Device 52 (Table VI) has a conversion efficiency of 12.7% when illuminated with 1873°K blackbody radiation while device 29 (Table IV) has a conversion efficiency of 14.7% when illuminated with 1873% Er $_2$ O $_3$  radiation. In both cases the value of CURD $\bar{O}$ P $\bar{T}$  is 5.0 amps cm $^{-2}$ .

TABLE VI  
Optimum Dimensions and Output Parameters of Devices  
Illuminated with 1873°K Black Body Spectrum\*

LI = 25 μm Incident Power = 9.8 Watt cm<sup>-2</sup> CURDOPT = 5.0 amps cm<sup>-2</sup>  
RCOMFAC = 2.8 × 10<sup>-14</sup> cm<sup>3</sup> sec<sup>-1</sup>

Device #	VSB (cm sec <sup>-1</sup> )	VST (cm sec <sup>-1</sup> )	LF (μm)	LP (μm)	XO (μm)	FMAXPOW <sub>2</sub> (watt cm <sup>-2</sup> )	EMACELL (g)	EMACOL	ETAABS	CF	VOC (volts)	CURDSC (amp cm <sup>-2</sup> )
52	0	0	150.3	224.3	508.5	1.241	50.07	.9935	.7508	.7532	.4416	3.730
53	10	10	170.1	264.7	520.2	1.214	48.85	.9861	.7532	.7439	.4395	3.714
54	100	100	234.1	377.8	530.8	1.029	41.30	.9258	.7552	.6912	.4259	3.496
55	500	500	221.2	366.6	321.1	.6705	28.81	.8184	.7052	.6104	.3807	2.886
56	1000	1000	157.9	262.7	179.5	.5070	23.65	.7927	.6496	.5760	.3420	2.573
57	0	10	152.5	229.3	518.0	1.216	48.96	.9861	.7528	.7451	.4398	3.762
58	0	100	154.3	234.2	526.0	1.040	41.77	.9262	.7544	.6968	.4272	3.493
59	0	1000	166.8	265.3	375.0	.0540	21.20	.6717	.7204	.5875	.3545	2.420
60	10	0	179.1	286.2	510.9	1.239	49.96	.9936	.7514	.7518	.4414	3.733
61	100	0	291.3	477.5	519.9	1.226	49.33	.9928	.7532	.7450	.4402	3.739

\* The FORTRAN variables given in this table are defined in Table XIV. The estimated error in values of FMAXPOW is 1% or less. The values in the Table are listed as they appeared in the computer program printout. Although the output values are generally inaccurate beyond the second decimal place, small difference between two corresponding output values for different values of input parameters will generally be accurate to the third or fourth decimal place.

## II. EXPERIMENTAL INVESTIGATIONS

### A. Introduction

The discussion of the experimental work will consist of the following:

- (1) a brief description of the device fabrication process; (2) a detailed description of investigations involving the fabrication process; (3) a discussion of the performance of devices that have been fabricated, and
- (4) a listing of the deficiencies which exist in devices that have been fabricated and a description of tests that have been carried out to isolate these deficiencies and measure their effects.

### B. Description of Device Fabrication Process

The steps involved in fabricating a TPV cell are given below.

1. An intrinsic germanium wafer is chemically polished on both sides.<sup>2</sup>
2. An insulating film is deposited on both sides of the wafer.
3. A pattern for the formation of the n contact is etched in the insulator on one side of the wafer.
4. Metal(s) for the n contact is vacuum evaporated on the wafer.
5. The metal(s) is etched so that it covers only the portion of the wafer on which the insulator has been etched. (See Figure 7.)
6. A pattern for the formation of the p contact is etched in the insulator.
7. Metal(s) for the p contact is vacuum evaporated on the wafer.

8. The metal(s) is etched so that it covers only that portion of the wafer on which the insulator has been etched for the p contact.

9. The contact metals are alloyed to the germanium. (See Figure 8.)

During the course of the experimental work some devices were fabricated according to the above procedure. A number of variations in this procedure were investigated, and a variety of insulating films and contact metals were investigated.

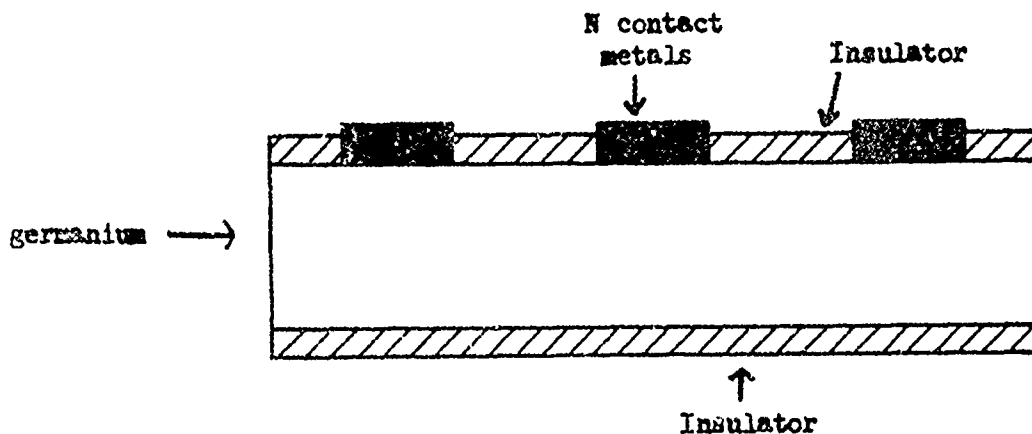


Figure 7. Partially Fabricated p-i-n Thermophotovoltaic Cell

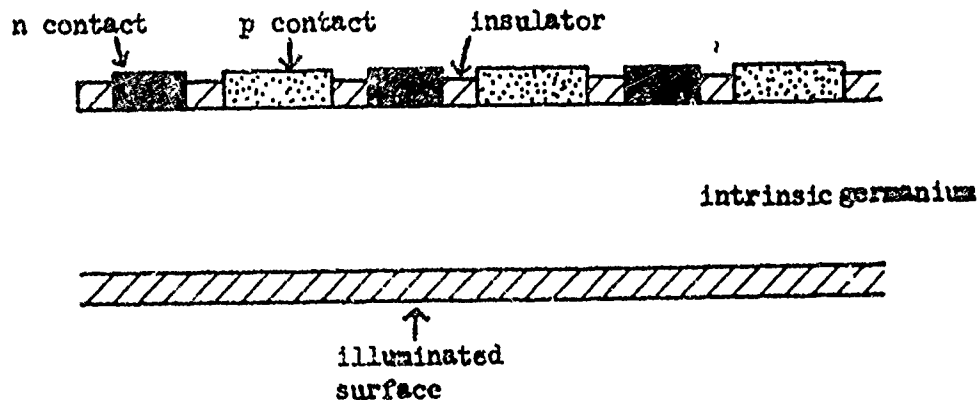


Figure 8. Completely Fabricated p-i-n Thermophotovoltaic Cell

C. Experimental Investigations of the  
Fabrication Process

1. Insulator deposition

The insulators which have been investigated are pyrolytically deposited silicon dioxide and vacuum deposited aluminum oxide.

Silicon dioxide deposition.-- It is desirable to carry out device processing at the lowest possible temperature in order to prevent diffusion of lifetime destroying impurities into the germanium bulk. Therefore, an investigation was carried out in order to determine the lowest possible temperature at which the silicon dioxide could be deposited. A reasonably fast deposition ( $900 \text{ \AA}/\text{min}$ ) could be obtained at a temperature as low as  $310^{\circ}\text{C}$ .

A method of device fabrication was proposed in Report No. 1<sup>1</sup> in which the p contact was formed before the n contact. Aluminum was to be used for the p contact. After the aluminum was deposited, etched and alloyed, silicon dioxide was deposited on top of the aluminum. Windows for n contacts were then etched in the silicon dioxide, and metals (gold and antimony) for the n contact were subsequently evaporated and alloyed. The necessity of etching the n contact metals was to be eliminated because of the insulating layer between the aluminum and the n contact metals.

The results of attempts to fabricate devices with the above described procedure were as follows: In cases where the silicon dioxide layer was deposited on top of the aluminum contact at  $360^{\circ}\text{C}$ , the p and n contacts were invariably shorted. Furthermore, the silicon dioxide invariably cracked on the aluminum once the thickness of the silicon dioxide exceeded  $2000 \text{ \AA}$ . Devices for which the silicon dioxide was deposited at  $425^{\circ}\text{C}$  were occasionally workable.

Aluminum oxide deposition.-- An investigation was carried out to determine if vacuum evaporated aluminum oxide could be used as an insulating layer between contacts. It was observed, however, that, while aluminum oxide appeared to cover the top of the aluminum contact well, it did not cover the contact edges.

Photoresist problems with SiO<sub>2</sub> films.-- The positive photoresist AZ-1350\* is generally used during the device fabrication. When this photoresist is used on pyrolytically deposited silicon dioxide, it is necessary to take certain precautions.

First of all, the developer which is normally used with this photoresist (AZ-1350 Developer\*) contains an abundance of sodium ions. Since silicon dioxide is highly permeable to sodium ions, and since it is feared that these ions will have a detrimental effect on the surface recombination velocity, it is desirable to use the developer XP-7110-1.\*

Secondly, AZ-1350 has a tendency not to stick to pyrolytically deposited silicon dioxide, and, therefore, it is necessary to take extra precautions to insure adhesion.

## 2. Contact formation

In order to avoid excessive leakage of minority carriers through the contacts, it is necessary that the contacts be very heavily doped and fairly thick. The requirement of low temperature processing rules out the use of high temperature diffusion techniques because of the danger of diffusion of lifetime destroying impurities into the germanium bulk. Heavily doped contacts can be obtained with alloying techniques, but in order to obtain sufficiently thick regrowth regions, it is necessary either to alloy at high temperatures or to deposit rather thick films

---

\* Mfg. by Shipley.

of contact metals (1 $\mu$ m or thicker). Experimental investigations have shown that the thickness of vacuum deposited films is limited because of the effects of surface tension in the films. The increased surface tension of thick films has two adverse effects: (1) There is a tendency for the films to ball up or develop craters during the alloying process. (2) The adhesion of the films is poorer.

n contacts

Kim<sup>4</sup> has investigated several combinations of metals for forming alloyed n contacts and has found that the best results were obtained when gold was used as a carrier with arsenic and antimony being used as dopants. For this reason investigations were carried out in which these metals were to be used to form alloyed n contacts. It was discovered that vacuum deposited films of gold and antimony adhered very poorly to germanium, and, therefore, it was impossible to etch these films without removing them from the germanium. Because of this adhesion problem, several attempts were made to build a device without having to etch the gold-antimony film. The first of these attempts is described on page .

The second attempt was identical to the first attempt except that the position of silicon dioxide on the aluminum contact pattern was omitted. Instead, a second layer of aluminum was evaporated and etched to cover the first layer of aluminum. After the gold-antimony film was evaporated, it was alloyed to the germanium at a temperature below the aluminum-germanium eutectic . It was hoped that the unalloyed aluminum film would not be affected by the gold-antimony layer on it during the alloying process. Then the alloyed gold-antimony film (which would stick to the germanium during the photo etching process) could be etched to separate the n contact

from the p contact. It was evident, however, that the gold-antimony film had interacted with aluminum film during the alloying process.

The proposed steps in the third attempt to fabricate a device were as follows: (1) Silicon dioxide would be deposited on both sides of a germanium wafer. (2) A pattern would be etched in the silicon dioxide on one side of the wafer through which the n contact would be formed. (3) Gold and antimony would be evaporated and alloyed to form the n contact. (4) The gold-antimony film would be etched so that it would remain only in those regions of the device on which the n contact pattern had been etched through the silicon dioxide. (5) A p contact pattern would be etched. (6) An aluminum film would be deposited and etched so that it would cover only the p contact region. (7) The aluminum would be alloyed to the germanium.

After the gold-antimony film had been alloyed [step (3)], however, large areas of balled-up gold-antimony alloy formed on the silicon dioxide. When step (4) was carried out, it was observed that the photoresist broke down before the thick balled-up regions could be completely etched.

An unsuccessful attempt was made to improve adhesion of gold to germanium by evaporating a mixture of gold and germanium simultaneously on a germanium wafer.

Eventually it was discovered that gold would adhere extremely well to germanium if the gold were evaporated immediately after the germanium surface had been subjected to an argon ion etch.\*

---

\*The ion etch is carried out at an argon pressure ranging from 50 microns to 10 microns while the vacuum system is pumping down the pressure. The duration of the ion etch is about 30 sec. The germanium wafer is in good electrical contact with a cathode that is maintained at a voltage of 600 volts D.C.

Several methods of "etching" the gold antimony films were investigated. These methods are described below:

Chemical etching.-- While chemical etching is procedurally complicated, it invariably produces sharp etches and can be used with relatively thick vacuum deposited films.

Ultrasonic "etching".-- Although gold sticks very well to ion etched germanium, it does not stick at all to silicon dioxide. Therefore step 5 of the procedure outlined in section B (page 24) can be carried out by removing the gold-antimony film from the silicon dioxide with a rigorous ultrasonic cleaning. Although this method of "etching" is procedurally simple, it has two disadvantages: (1) It does not produce as sharp a pattern as chemical etching. (2) It tends to become less satisfactory as the gold-antimony film becomes thicker. This is because the adhesion of the film to germanium becomes poorer.

Photoresist lift-off "etching".-- A third method of "etching" can be carried out as follows: (1) A photoresist pattern is developed on the wafer. (2) The metal film is deposited. (3) The photoresist and the metal film on top of it are stripped from the wafer, leaving a metal pattern which complements the photoresist pattern.

This method of etching has three disadvantages: (1) It does not produce as sharp a pattern as chemical etching. (2) It does not work for films that are too thick. (The photoresist won't lift off thick films.) (3) It is inherently dirtier than chemical or ultrasonic etching.

The advantage of photoresist lift-off etching is that the problem of etching the second metal contact pattern without attacking the first is eliminated.

A device was built using lift-off etching techniques. The processing steps were as follows: (1) Silicon dioxide was deposited on both sides of a wafer. (2) Both p and n contact patterns were etched in the wafer. (3) A photoresist pattern was developed which left only the p contact region uncovered. (4) An aluminum film was deposited. (5) The photoresist and the aluminum film above it were stripped from the wafer. (6) A photoresist pattern was developed which left only the n contact region uncovered. (7) Gold and antimony were deposited after an ion etch. (8) The photoresist and the gold-antimony film above it were stripped from the wafer.

Arsenic doped contacts.-- Investigations were carried out in which arsenic was used with gold or gold and antimony to form alloyed n contacts. Two noteworthy observations were made: (1) Arsenic-gold and arsenic-antimony-gold film tended to stick fairly well to germanium, provided that the arsenic was evaporated first. However, the films did not stick as well as gold antimony films of comparable thickness which had been deposited after an argon ion etch. (2) Alloyed arsenic-gold films tended to ball up much more readily than arsenic-antimony-gold films of comparable thickness.

Other combinations of metals have been investigated for n contacts. These investigations are discussed later.

#### p contacts

Aluminum has been thoroughly investigated as material for forming p contacts because of its very high solid solubility in germanium.

Thick films of aluminum (of the order of 10  $\mu\text{m}$ ) have been investigated because of the need to form thick germanium regrowth regions during

the alloying process. Because of the long time required to etch these films, the photoresist would break down, and pin holes would develop in the aluminum film. Experiments were conducted with various etchants and etching techniques to eliminate this problem. It was determined that photoresists would hold up satisfactorily if the film was etched in warm aluminum etch\* (approximately 40°C).

Experiments have been conducted to determine if the adherence of aluminum films could be improved by an ion etch, (although aluminum films generally stick well without ion etches). The results indicate that the adherence of aluminum is improved slightly by an ion etch.

Other metals and combinations of metals have been investigated as materials for forming p contacts. The results of these investigations as well as the results of more detailed investigations of aluminum will be discussed in the following section.

#### Alloying

An extensive series of investigations was carried out in which various metal films and combinations of metal films were tested for possible use as p or n contacts. The metallic films were alloyed to the germanium at various temperatures and were angle-lapped and stained. The quality of the films was judged on the basis of the smoothness of the crystal regrowth region in the germanium.

Junction staining solution.-- Some preliminary tests were carried out in order to select a suitable junction staining solution. Aluminum balls were alloyed to germanium substrates to form thick heavily doped regrowth regions in the germanium. The substrates were lapped through the alloyed region and stained with various solutions. The best results were

---

\*The composition of aluminum etch is given in Table VIII.

obtained with a 30 second stain in a solution consisting of 20 parts HF to one part  $\text{HNO}_3$ .

Alloying technique.-- All metallic films were vacuum deposited on chemically polished germanium substrates which had been cleaned ultrasonically in methanol, acetone and trichlorethylene and exposed to an argon ion etch.

The alloying was done in an alloying system in which the substrate was placed between two carbon heater strips. The heater strips could be heated independently, and thus the sample could be alloyed in a temperature gradient. The spacing between heater strips was about a half millimeter. The sample was placed on the lower heater strip with the surface on which the metallic film had been evaporated facing upward. The temperature of the upper strip was maintained about  $100^\circ\text{C}$  higher than that of the lower strip.\* The alloying temperatures given in the following discussions are those of the lower substrates.

The samples were heated at a rate of about  $10^\circ\text{C sec}^{-1}$ . A cooling rate of about  $5^\circ\text{C sec}^{-1}$  was begun immediately after the alloy temperature had been reached. All alloying was done in hydrogen.

Aluminum films.-- Aluminum films approximately one micron thick were deposited on germanium substrates. The films were alloyed at temperatures of  $450^\circ\text{C}$ ,  $500^\circ\text{C}$  and  $700^\circ\text{C}$ . The samples were angle-lapped and stained. In the samples which were alloyed at  $500^\circ\text{C}$  and  $700^\circ\text{C}$ , the regrowth regions were extremely irregular, and there was no perceptible

---

\* According to EerNisse<sup>3</sup> the regrowth region in the germanium substrate tends to be smoother when the temperature of the alloy melt is maintained above that of the germanium substrate.

regrowth in the sample which was alloyed at 450°C.

There was also a tendency for craters to form on the alloyed aluminum film. There was no perceptible regrowth in germanium regions under these craters.

Indium films.-- An indium film approximately one micron thick was deposited on a germanium substrate and alloyed at 650°C. The film balled up badly during the alloying process, and regrowth was visible only under the balled up regions.

Aluminum on indium films.-- Indium films (approximately one micron) followed by aluminum films (approximately one micron) were deposited on germanium substrates. The films were alloyed at 650°C, 500°C, 450°C and 350°C. The regrowth region of the film alloyed at 650°C was fairly smooth, but it got progressively more irregular for the films alloyed at 500°C and 450°. The regrowth region was quite smooth for the film alloyed at 350°C. This was probably due to the fact that the alloying temperature was below the germanium-aluminum eutectic (424°C), and, therefore, the aluminum film did not liquify during the alloying process.

The "cratering" effect described in the discussion of aluminum films also occurred for these films. The craters tended to get progressively smaller at lower temperatures and were imperceptible for the film alloyed at 350°C.

Antimony on gold films.-- Gold films (approximately one micron) followed by antimony films (approximately one half micron) were evaporated on germanium substrates. The films were alloyed at 700°C and 525°C. The films balled up badly during the alloying processes, and regrowth was visible only under the balled up regions.

Antimony films.-- About three microns of antimony were evaporated on a germanium substrate and alloyed at a temperature of  $700^{\circ}\text{C}$ . The antimony balled up very badly during the alloying process, and no regrowth was visible in the germanium.

Tin-antimony-tin films.-- Some samples were prepared with a vacuum deposited film consisting of two layers of tin with a layer of antimony between them. The first and second layers of tin were approximately one half and one micron thick, and the antimony layer was approximately one half micron thick. The samples were alloyed at  $475^{\circ}\text{C}$  and  $650^{\circ}\text{C}$ . The regrowth regions were quite smooth and regular.

Conclusions.-- The most promising junctions for p contacts were obtained with the indium-aluminum films. The most promising junctions for n contacts were obtained with the tin-antimony-tin films. An attempt was made to fabricate a device using these films. It was discovered, however, that the adhesion of the films was not good enough.

An attempt was made to form tin-antimony-tin contacts on a device by alloying the film before etching it. Silicon dioxide was deposited on both sides of a wafer and was etched on one side to form an n contact pattern. A tin-antimony-tin film was evaporated and alloyed. But during the alloying process, the film balled up badly on the silicon dioxide, and apparently the surface tension created in the balled up regions on the silicon dioxide was large enough to cause the film to also ball up in the contact region.

Further investigations need to be carried out to determine the maximum thicknesses of indium-aluminum films and tin-antimony-tin films that will stick well enough to germanium to withstand ultrasonic cleaning and photoprocessing.

### Contact buildup

Since the thermophotovoltaic cell is designed for very high intensity illumination, rather large currents will be collected at the contacts; and, consequently, it is necessary that the resistance in the contact fingers be quite low. Therefore, investigations were carried out in which the resistance of the contact fingers was reduced by plating relatively thick (10-20 micron) films of gold on the contacts.

Attempts were made to plate gold directly on the alloyed aluminum and gold-antimony contacts of a completed device. The gold plating on the aluminum did not stick at all. The gold plating on the gold-antimony contact appeared to stick reasonably well, but the plating on the gold-antimony fingers bridged over to the aluminum fingers in several places.

The following method of building up the contacts satisfactorily eliminated the bridging over problem and permitted a buildup of both aluminum and gold-antimony contacts: (1) Very thin chrome and gold films were evaporated over the contact surface of the device. (2) A relatively thick gold film was electroplated on the vacuum deposited gold film. (3) The chrome-gold film was then etched to separate the P and N contacts. The chrome film was evaporated to form an adhesive layer with the aluminum; and the gold film was evaporated subsequently without breaking vacuum in order to prevent oxidation of the chrome film and thus insure the adhesion of the electroplated gold film. It is desirable to build up the contacts with electroplated rather than evaporated gold, because thick films of evaporated gold would produce an appreciable amount of surface tension. This surface tension would cause stresses in the germanium which could significantly reduce lifetime.

### 3. Fabrication problems

Compatibility of etchants and processing chemicals.-- A variety of chemicals and etchants are used in the process of fabricating a device. Some of the etchants which are quite satisfactory for etching the metal or insulator for which they are meant will attack other areas of the device. The fabrication process must be carried out in such a way that this doesn't happen. Table VII lists some of these chemicals and etchants and their effects on metals and insulators that are used in the fabrication process. The compositions of the etchants listed in Table VII are given in Table VIII.

Problems with gold contacting aluminum.-- The following process was used to fabricate the devices which were evaluated in the tests in section II-D: (1) Silicon dioxide was deposited on both sides of a wafer. (2) A pattern for n contacts was etched in the silicon dioxide. (3) A gold-antimony-gold\* film was deposited and etched to form the n contact. (4) A pattern for p contacts was etched in the silicon dioxide. (5) An aluminum film was deposited and etched to form the p contact. (6) The contact metals were alloyed to the germanium.

A problem occurred in step (5). Normally it is necessary to heat the device to a temperature of about 100°C for a period of about 30 minutes during the photoetching process. This heating period caused the aluminum to react with the gold. A method of photoprocessing without heating the device was developed in order to eliminate this effect.

---

\*The film consisted of two layers of gold with a layer of antimony between them.

TABLE VII

Effect of Chemicals and Etchants on Metals and Insulators

Chemical & Etchants	Metals & Insulators									
	Germanium	Silicon Dioxide	Aluminum Oxide	Aluminum	Indium	Gold	Antimony	Arsenic	Tin	Chrome
Silicon Dioxide Etch	4	1		1						
Aluminum Etch	4	4	1	1	1	4	3			
Gold Etch	2	4		1A		1	4			
Antimony Etch	1	4		2	1	1	1	1	1	
Chrome Etch		4				4				1
Nitric Acid	4	4		2	1		2		1	
J-100	4	4	4	4		4	3			
Water										2A

1. Etches rapidly.
- 1A. Does not attack aluminum but lifts of the aluminum by attacking the germanium surface under the aluminum film.
2. Etches slowly
- 2A. Causes flaking of film after several days immersion.
3. Has a discoloring effect.
4. Has no apparent effect.

TABLE VIII

Etchants used in Device Fabrication

Silicon Dioxide Etch:	104 ml Hydrofluoric acid
	454 gm Ammonium Fluoride
	682 ml Water
Aluminum Etch:	380 ml Phosphoric Acid
	15 ml Nitric Acid
	75 ml Acetic Acid
	25 ml Water
Gold Etch:	27 gm Iodine
	60 gm Potassium Iodide
	600 ml Water
Antimony Etch:	3 parts Nitric Acid
	1 parts Hydrochloric Acid
	6 parts Water
Chrome Etch:	27 gm Cerium Sulfate
	100 ml Nitric Acid
	400 ml Water

#### 4. Heat sink fabrication and device mounting

A photograph of a finished device mounted on a heat sink is shown in Figure 9. The interior of the heat sink is hollow. Cooling water enters and exits through the openings at opposite ends of the heat sink. The portion of the heat sink under the device is milled to a thickness of 1/16 inch. The milled surface is left unfinished to facilitate the conduction of heat between the surface and the circulating water. The heat sink is anodized in sulfuric acid to form an insulating layer of aluminum oxide approximately 5  $\mu$ m thick. The milled out portion is sealed at the bottom with an aluminum block which is epoxied on with stycast 2850FT\*. Banana jacks are soldered on two copper contact plates which are epoxied on opposite sides of the heat sink with Stycast 2850FT\*.

The device is epoxied to the heat sink with Stycast 2850FT\* used with the catalyst 24 LV. First of all, the device is mounted (the illuminated surface facing downward) on a glass slide with beeswax. The glass slide provides mechanical support. The device is then epoxied to the heat sink with the p and n contact pads extended over opposite edges of the heat sink. After the epoxy has cured the glass slide is removed by melting the beeswax, and the beeswax is removed with trichlorethylene. Finally the contacts on the device are soldered to the contact plates with Indalloy Solder #8 used with Flux #2.\*\*

---

\* Manufactured by Emmerson Cumming.

\*\* Manufactured by the Indium Corporation of America.

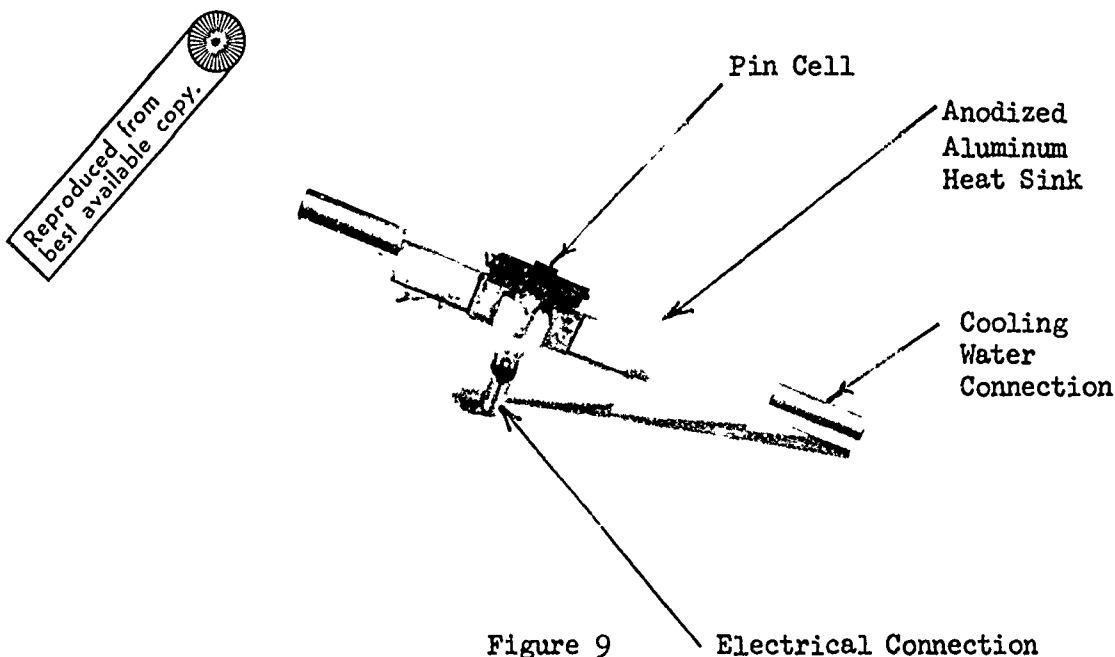


Figure 9  
p-i-n Cell Mounted on Water  
Cooled Heat Sink

5. Evaluation of heat sink performance.

The following experiment was carried out to estimate the degradation in the performance of heat-sinked cells due to the heating effect of the 9.95 watt-cm<sup>-2</sup> illumination source: A shutter was inserted between the cell and the illumination source to prevent heating of the cell. The I-V characteristics of the cell were monitored on a curve tracer. A series of traces on the curve tracer was photographed immediately after the shutter was removed. The effect of heating could be determined by observing the degradation in the I-V characteristics on the photograph of the traces.

In cases where there was no fluid circulating through the heat sink, a very significant degradation occurred in the cell performance. In cases where there was water circulating through the heat sink, however, the degradation was practically imperceptible.

#### D. Performance of Fabricated Devices

Some devices were fabricated with the process outlined pages 24 and 25. The open circuit voltages of each device was measured in a sample holder in which the illuminated surface was faced downward on a glass slide. A tungsten lamp illuminated the sample through the glass slide with an incident intensity of  $0.7 \text{ watts/cm}^2$ . No measurements were made to determine what percentage of the incident light was absorbed by the sample.

The results of the open circuit voltage measurements are shown in Table IX. The Table also lists the unique characteristics of each device.

Two note worthy observations can be made from the data in Table IX: (1) The quality of the device generally improves as the film thickness (especially the thickness of the n-contact films) is increased. (2) The quality of devices alloyed at temperatures at or above  $550^\circ\text{C}$  is better than that of those alloyed below  $550^\circ\text{C}$ .

The open circuit voltage of device #4 was measured again with the  $0.7 \text{ watt/cm}^2$  tungsten lamp being replaced with a  $9.95 \text{ watt/cm}^2$  tungsten lamp. The measured open circuit voltage was 0.28 volts.

Devices #1, 4 and 6 in Table IX were mounted on heat sinks. Because of problems encountered with breakage during processing, the active area of device #1 was reduced to  $0.6 \text{ cm} \times 0.55 \text{ cm}$ . Problems were encountered with the adhesion of electroplated gold films on devices #1 and 4. As a result the performance of these devices was significantly degraded after they were mounted on the heat sinks.

The I-V characteristics of device #6 are shown in Figure 10. The  $9.95 \text{ watt/cm}^2$  illumination source is used. The short circuit current

TABLE IX

Open Circuit Voltage Output of Fabricated Devices  
0.7 w/cm<sup>2</sup> Tungsten Illumination

Device #	Active area (cm x cm)	Total Thickness of Gold Films (Å)	Thickness of Antimony Film (Å)	Thickness of Aluminum Film (Å)	Alloying Temperature (°C)	Open Circuit voltage (volts)
1*	0.6 x 1.5	300	300	1500	450	0.10
2	0.6 x 1.5	250	250	1500	450	0.06
3	0.55 x 0.30	1000	750	6000	450	0.12
4*	0.55 x 0.30	1000	750	6000	550	0.19
5	0.55 x 0.30	500	250	12000	550	0.165
6*	0.55 x 0.30	500	250	12000	550	0.16
7	0.5 x 0.30	500	250	6000	700	0.14

\* Mounted on heat sinks

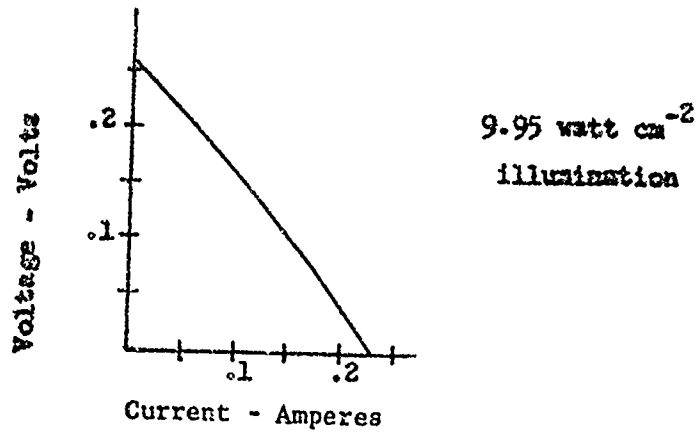


Figure 10. Voltage Curves for Device #6 (See Table IX)

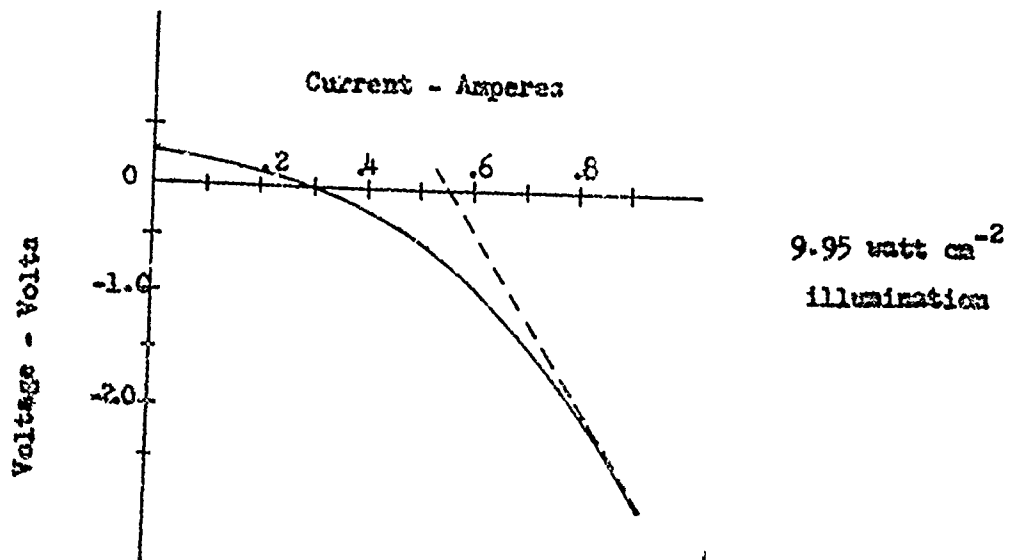


Figure 11. Current - Voltage Curve for Device #6 Reverse Bias Applied (See Table IX).

obtained is 240 ma. Since the active area of the device is 0.55 cm x 0.30 cm (See Table IX ), the short circuit current collected per unit area is 1.5 amp cm<sup>-2</sup>.

An attempt was made to estimate the maximum attainable short circuit current. A reverse bias was applied to the device, while it was illuminated by the 9.95 watt cm<sup>-2</sup> source. The reverse characteristics appeared to approach an asymptote. (See Figure 11.) The asymptote intersected the current axis at 550 ma. This current is presumably the maximum collectable current of the device. The current collectable per unit area for the 0.55 cm x 0.30 cm device is 3.3 amp.cm<sup>-2</sup>.

#### E. Investigation of Deficiencies in Devices

The deficiencies in the performances of the devices that have been fabricated can be attributed to any combination of the three following factors: (1) excessive bulk recombination; (2) excessive surface recombination; (3) faulty contacts. The following discussion describes how the relative importance of each of these deficiencies is evaluated.

##### 1. Contacts deficiencies

A series of samples was prepared according to the following procedure:  
(1) Silicon dioxide was deposited on both sides of a polished intrinsic germanium wafer. (2) A pattern of dots was etched through the silicon dioxide on one side of the wafer. (3) An aluminum film was deposited over

half the surface on which the dot pattern had been etched.

(4) Metal films for n contacts were deposited on the other half of the wafer on which the dot patterns had been etched. (5) The aluminum and n contact films were etched to form a complementary pattern to the silicon dioxide pattern. (I.e., the metal films patterns consisted of dots which covered the areas of the surface on which the silicon dioxide film had been etched.) (6) The aluminum and n contact films were alloyed simultaneously.

The open circuit voltage of the devices fabricated according to the above procedure was measured while the unprocessed surface of the device was illuminated with the  $0.7 \text{ watt/cm}^2$  source. The testing procedure was exactly the same as that used to obtain the results shown in Table IX. The results of the measurements are summarized in Table X. The following conclusions can be drawn from these results: (1) In general the open circuit voltages obtained for devices with the arsenic-doped contacts is better than that obtained for devices without arsenic-doped contacts. (2) The open circuit voltage seems to hit an upper limiting value of 0.20 volts.

## 2. Lifetime damage due to silicon dioxide deposition

A series of tests was carried out to evaluate the effect of silicon dioxide deposition on the bulk and surface lifetime of devices. Three germanium strips were cut from an intrinsic wafer which had been polished on both sides. Silicon dioxide was deposited on one side of one strip and on both sides of another. Four gold contacts were then evaporated on each strip to form the type of structure shown in Figure 12. The portion of the contact on the rough edge was for the purpose of forming a good ohmic contact; and the portion of the contact on the polished

TABLE X

## Open Circuit Voltage Output of Dot-Pattern Devices

Device #	Thickness of Aluminum Film (A)	n Contact Material*	Thickness of n Contact Material Film (R)	Alloying Temperature ( $^{\circ}$ C)	Open Circuit Voltage (volts)
1	4500	Au	360	435 $^{\circ}$ C	0.125
		Sb	400		
		Au	120		
2	4500	Au	360	520 $^{\circ}$ C	0.17
		Sb	400		
		Au	120		
3	4500	As	130	435 $^{\circ}$ C	0.195
		Sb	130		
		Au	700		
4	4500	As	130	520 $^{\circ}$ C	0.20
		Sb	130		
		Au	700		
5	4500	As	200	435 $^{\circ}$ C	0.20
		Sb	500		
		Au	10,000		
6	4500	As	200	435 $^{\circ}$ C	0.15
		Sb	500		
		Au	3,000		
		Sb	20,000		

\*The n contact films for a device are listed in the order in which they were evaporated.

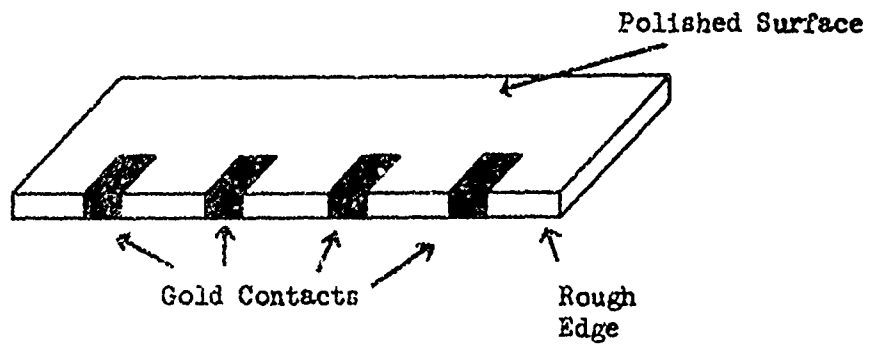


Figure 12. Sample Used to Test Effect of Silicon Dioxide Deposition on Lifetime

surface was for making contact with a probe.

The sample was illuminated, and the excess carrier concentration due to the illumination was measured by measuring the conductivity of the substrate. (See Figure 13.) Since the gold contacts were not perfectly ohmic, the conductivity was measured by a four point probe technique. A fixed current flowed through the outer probes, and the voltage drop was measured across the inner probes with a high impedance volt meter. Since the germanium substrates were intrinsic, the ratio of excess carrier concentration to intrinsic carrier concentration was given by the ratio of the voltage drop without illumination to the voltage drop with illumination.

The results of the measurements are summarized in Table XI. The test fixture and illumination source are the same as those used to obtain the results shown in Tables IX and X.

The following conclusions can be drawn from the results in Table XI:  
(1) The deposition of silicon dioxide appears to degrade the bulk and/or surface lifetime. (2) The silicon dioxide film enhances the absorption of useful illumination. (3) The effect of depositing silicon dioxide on both sides of the wafer is not significantly different from the effect of depositing it on one side only.

### 3. Determination of the dominant source of recombination

Theoretical investigations have shown that surface recombination velocity is smaller for accumulated or depleted surfaces than for flat band surfaces. An experiment was carried out in which the surface recombination velocity of a germanium substrate was varied by varying the surface potential. The substrate was prepared like the sample shown in Figure 12 with silicon dioxide films deposited on both sides.

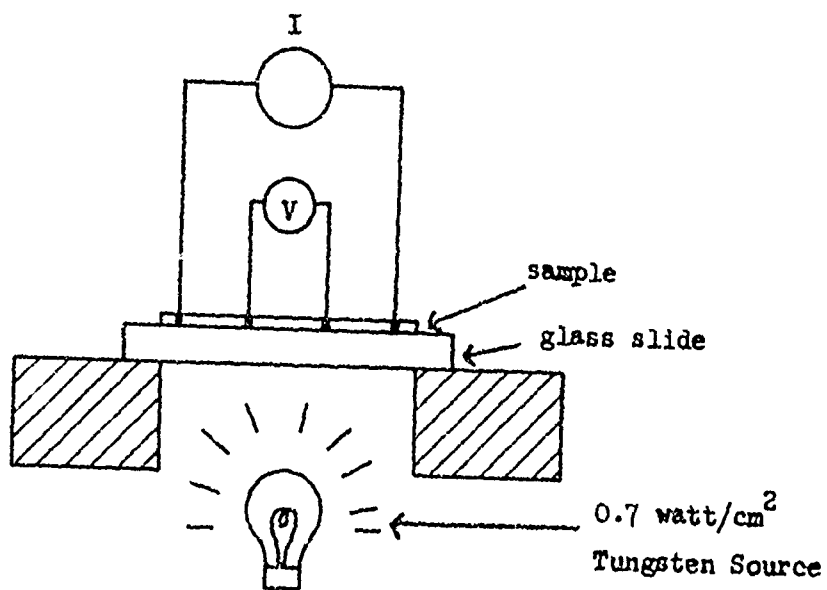


Figure 13. Apparatus Used to Test Effect of Silicon Dioxide Deposition on Lifetime

TABLE XI

Effect of Silicon Dioxide Deposition on Excess Carrier Concentration

Sample #	Description	Relative Excess Carrier Concentration ( $n/n_i$ )
1	No silicon dioxide on either side	110
2	Silicon dioxide on one side; side without silicon dioxide was illuminated	37
2	Silicon dioxide on one side; side with silicon dioxide was illuminated	46
3	Silicon dioxide on both sides	40

Transparent but electrically conducting films of aluminum were deposited on both sides of the substrate. The aluminum films were electrically isolated from the gold contacts and the germanium substrate.

The conductivity of the samples was measured with the apparatus shown in Figure 13, but with two modifications: (1) The 0.7 watt cm<sup>2</sup> tungsten source was replaced with a low intensity source in order to prevent heating the substrate. (2) A D.C. bias was applied to the transparent aluminum plates with respect to one of the voltage contacts.

The results of the measurements are shown in Table XII.

TABLE XII

Relative Conductivity as a Function of Surface Bias

Bias (volts)	Relative excess carrier concentration $(\frac{n}{n_i})$
10	0.11
5	0.15
0	0.22
-5	0.24
-15	0.40
-30	0.49
-41	0.72

The change in conductivity resulting from the surface charge layer induced by the bias was appropriately compensated for. The following observations can be made: (1) The rate of recombination on the surface is greater than the rate of recombination in the bulk. The excess carrier concentration at -41 volts is more than three times as great as that at 0 volts. (2) Contrary to theoretical predictions the excess carrier concentration for accumulated n-type surfaces (positive bias) does not increase with increasing bias. Furthermore the excess carrier concentration for accumulated p-type surfaces (negative bias) does not increase with increasing bias as fast as it should. Both of these effects are probably due to the drift of ions in the unannealed silicon dioxide film.

#### 4. Conclusions

The following conclusions can be drawn from the tests which were carried out to investigate the deficiencies of the devices. (1) For devices whose open circuit output voltage is well below 0.20 volts<sup>\*</sup>, the dominant deficiency is faulty contacts. (2) For devices whose open circuit voltage is nearly equal to 0.20 volts<sup>\*</sup>, the dominant deficiency is excessive surface recombinations. If bulk recombination was the dominant recombination mechanism, the measurements summarized in Table XII would have been independent of bias voltage. These conclusions can be collaborated with a mathematical expression which may be used to roughly approximate the excess carrier concentration at the junctions of a p-i-n thermophotovoltaic cell in terms of the open circuit voltage:

$$\frac{n}{n_i} = \exp \frac{eV}{2kT}$$

For  $V = 0.20$  volts and  $T = 300^\circ\text{K}$ ,  $n/n_i = 47$ . This compares reasonably well with the values of 46 and 40 obtained with devices 2 and 3 in Table XI.

---

\* This value of open circuit voltage is for samples illuminated with the 0.7 watt  $\text{cm}^2$  source with the same test fixture used to obtain the results in Tables IX, X, and XI.

### III. CONCLUSIONS AND RECOMMENDATIONS

As we have pointed out in our description of the experimental results, the performance of the devices which were fabricated falls far short of the performance which was predicted for devices with optimum physical parameters. The primary reasons for this are:

1. High surface recombination velocity
2. High bulk recombination
3. Poor junctions

Any future program which is directed toward the improvement of p-i-n planar photovoltaic cells should take these points into consideration. The surface recombination can be reduced through appropriate annealing procedures after the deposition of the insulating film. The alloying problems which have been discussed can be solved either by using appropriate alloying techniques or by the use of ion implantation to form the  $n^+$  and  $p^+$  contacts. The problem with bulk recombination reduction during processing can be eliminated by using a fabrication procedure which keeps the maximum processing temperature below  $300^{\circ}\text{C}$ . In that case very little degradation should occur in the bulk lifetime.

A maximum conversion efficiency of 14.7% was computed for an optimized device operating with illumination from an  $1873^{\circ}\text{K}$  erbium oxide source. Nearly half the energy radiated from such a source is carried by photons whose energy is below that of the germanium band gap. The use of a reflective coating which will return these photons to the source can lead to significant improvement in the operating efficiency. Future work should

include the fabrication of cells which have such reflective coatings.

Little work has been done on the present study with regard to heat sinking of the device. It is necessary that such heat sinking be accomplished because of the very rapid degradation of the device characteristics with an increase in cell temperature. Heat sinking of a p-i-n planar cell is more difficult than for a standard p-n junction cell because of the fact that the electrical contacts are both on the same surface as the heat sink, and one must simultaneously obtain the electrical isolation and good thermal contact to the surface. Any future work should include a program to minimize the temperature drop across this interface.

If the above mentioned problems can be solved, and all indications are that they can, the result should be a thermolphotovoltaic cell with relatively high conversion efficiency.

REFERENCES

1. R. J. Schwartz, "A Theoretical and Experimental Investigation of Planar PIN Thermophotovoltaic Cells", Annual Report, TR ECOM-0129-1, Contract No. DAABC7-70-C-0129, August, 1971.
2. A. Reisman, R. Rhor, "Room Temperature Chemical Polishing of Ge and Ga As", J. Elec. Chem. Soc., Vol. 111, p. 1425, 1964.
3. N. Goldsmith, F. Kern, "The Deposition of Vitreous Silicon Dioxide Films from Silane", RCA Review, p. 153, March, 1967.
4. C. W. Kim, P-I-N Thermo-photo-voltaic Diode, Ph.D. Thesis, Purdue University, 1968.
5. E. P. ErNisse, Temperature Gradients in Semiconductor Alloying Technology, Ph.D. Thesis, Purdue University, 1965.
6. W. van Rousbroek, W. Shockley, "Photon-Radiative Recombination of Electrons and Holes in Germanium", Physical Review, Vol. 94, p. 1558, June 15, 1954.

## APPENDIX

In this appendix the ADOP program will be described in some detail. The input parameters and the printed output will also be described.

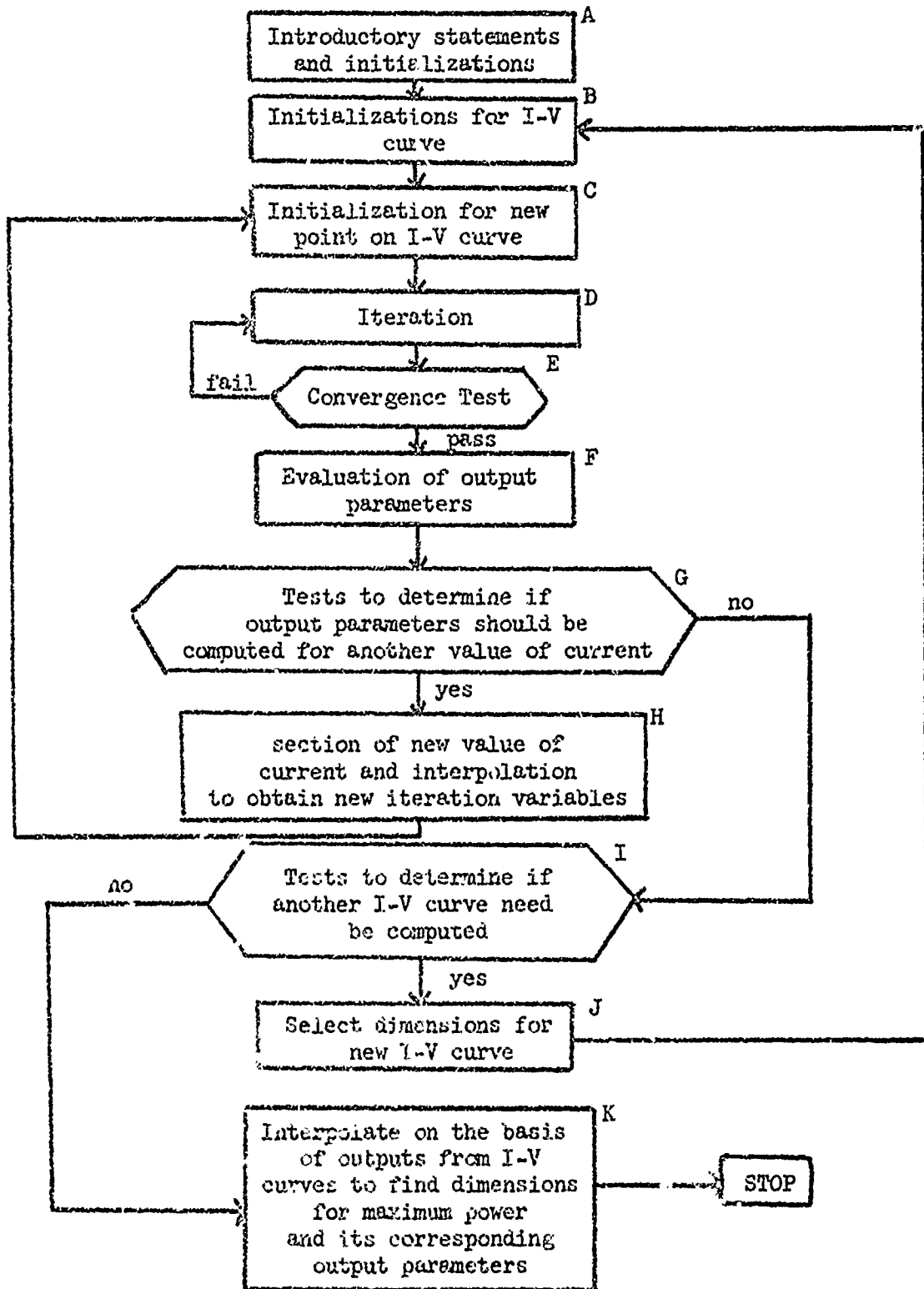
### Description of the Program

The program is described very briefly in the flow chart shown on page 58 . First of all the input values are set and preliminary computations and initializations are made (Box A). These input values include an initial guess of the dimensions of the device for which the maximum power will occur. The input current is initially set equal to zero (Box B). After additional initial computations done in Boxes B and C, the open circuit voltage is evaluated (Boxes D, E and F). In order to evaluate the output voltage, a boundary value problem must first be solved.\* This problem is solved in the computer program by successive over-relaxation. In the successive over-relaxation process an iteration (Box D) is carried out in which a new and better estimate of the solution of the boundary value problem is obtained from an original estimate. Then a convergence test is carried out to determine if the new estimate is sufficiently close to the solution of the boundary value problem. If not, the new estimate is used in the iteration process to obtain a still better estimate. By repeated iterations and convergence tests, the estimate is successively improved until the convergence test is finally passed.

---

\*The theoretical formulation of the boundary value problem and a detailed description of the portion of the computer program in which it is solved is included in Report No. 1<sup>1</sup>.

ADOP PROGRAM



The solution of the boundary value problem is then used to compute the output voltage and other output parameters (Box F).

Once the open circuit voltage is computed, a new value of current is selected (Box H); and the computations made in Boxes C, D, E and F are repeated to obtain the output voltage for this current. This process of selecting new values of current and evaluating the corresponding values of voltage is repeated until a sufficient number of values are obtained to provide very good estimates of the short circuit current and the maximum power.

After it has been determined that the short circuit current and the maximum power can be satisfactorily estimated (Box G), a new set of dimensions is selected for the device (Box J). The process of obtaining enough points on the I-V curve to estimate the maximum power and the short circuit current is repeated for the new set of dimensions.

This process of selecting new dimensions and evaluating the output parameters for these dimensions is systematically repeated. The dimensions are selected in such a way that they tend to be close to those dimensions for which maximum power will occur.\*

After it has been determined that the output parameters have been evaluated for a sufficient number of sets of dimensions (Box I), the maximum power and the dimensions for which maximum power will occur are determined by means of an interpolation process. A quadratic function of the form

$$P = A_0 + A_1 l_n + A_2 l_p + A_3 x_o + A_{11} l_n^2 + A_{22} l_p^2 + A_{33} x_o^2 + 2A_{12} l_n l_p + 2A_{13} l_n x_o + 2A_{23} l_p x_o$$

---

\*The dimensions which are varied are the width of the n contact ( $l_n$ ), the width of the p contact ( $l_p$ ), and the thickness of the device ( $x_o$ ). These dimensions must be varied in discreet increments. (See Report No. 1.)

is fitted to the values of output power associated with ten appropriately selected sets of dimensions. In the above equation  $P$  is the power output and the  $A$ 's are constants. Note that since there are ten  $A$ 's, ten equations (which come from the ten sets of dimensions) are needed to evaluate these  $A$ 's. Once the  $A$ 's are evaluated, the values of  $l_n$ ,  $l_1$ , and  $x_0$  which maximize  $P$  are determined, and finally the maximum power is obtained.

A number of other parameters (such as open circuit voltage and short circuit current) are obtained from quadratic interpolations for the dimensions at which maximum power occurs.

#### Input parameters

The input parameters are listed in the three categories which are defined below: physical parameters--physical values which are needed to evaluate the performance of the device; dimension parameters--numerical values which define the dimensions of the device; program parameters--numerical values which control the speed and accuracy of the program and the amount of detail in the output.

#### Physical parameters

The physical parameters which are listed in statements 1650-2100 of the ADOP program are described in Table XIII. The generation rate of hole-electron pairs as a function of distance from the illuminated surface is read in at statement 4250.

TABLE XIII

LIST OF PHYSICAL PARAMETERS

FORTRAN Name	Physical Symbol(s)	Comments
KTOE	$kT/e$	<u>(kT over e)</u>
DP	$D_p$	hole diffusion coefficient
DN	$D_n$	electron diffusion coefficient
NI	$n_i$	intrinsic carrier concentration
RCOMFAC	$r$	<u>recombination factor</u>
VSB	$V_{S.B}$	Surface recombination velocity on <u>bottom or unilluminated surface.</u>
VST	$V_{S.T}$	surface recombination velocity on <u>top or illuminated surface</u>
VGAP	$V_G$	(energy gap voltage)
CURDOPT		<u>(optimum current density)</u>  The current collected per unit area of illuminated surface if every photon capable of generating a hole-electron pair is absorbed and if every optically generated hole- electron pair is collected.

Dimension parameters

The dimension parameters which are given in statements 3100-3400  
can be described concisely in the following equations:

- (1)  $LN = 2 * NLN1 * K$
- (2)  $LP = 2 * NLP1 * K$
- (3)  $XO = NXO1 * H$
- (4)  $LI = NL11 * K$
- (5)  $\left. \begin{array}{l} \text{minimum} \\ \text{value of} \\ XO \end{array} \right\} = (NXOMIN + 1) * H$

where

- LN = width of n contact
- LP = width of p contact
- XO = thickness of device

The fortran variables NLN1, NLP1, NXO1, NL11 and NXOMIN are integers. The variables H and K are real numbers which specify increment sizes in centimeters. (See Report No. 1.<sup>1</sup>) The dimensions are constrained to values which are integral factors of these increments. In the ADOP program the dimensions of the device are varied by systematically varying the values of NLN1, NLP1 and NXO1 (Box J of the flow chart). The initial guess of the dimensions for which maximum power occurs is determined by the initially specified values of NLN1, NLP1 and NXO1.

In some cases the optimum thickness of a device will be much thinner than the minimum thickness attainable in practice due to limitations in technology. Therefore the program has been adapted to optimize the device under the constraint that XO will have a specified minimum attainable value. This value can be specified by appropriately choosing NXOMIN and H in equation (5).

The time required to run the ADOP program can be reduced by choosing the largest possible values for H and K<sup>1</sup>. On the other hand, the accuracy

of results obtained increases with decreasing values of H and K.<sup>1</sup> Experimental runs were carried out for which the physical parameters and the device dimensions were held constant as H and K were varied. The error in the value of maximum power was made negligible by choosing sufficiently small values of H and K. The error in the value of maximum power obtained for larger values of H and K could then be estimated by comparing the maximum power obtained with larger values of H and K with that obtained with the small values of H and K. For values of H and K used to obtain the results in Tables I through VI the estimated error is 1% or less.

#### Program parameters

A discussion of program parameters is of little value unless one wishes to use the program. In this case a detailed description of the program will be needed. A document providing such a description will be prepared at a later date.

#### Printed output

Table XIV lists and describes the FORTRAN variables that appear in the printed output in the order in which they appear.

The printout can be divided into two parts. The first part gives the output for a given set of dimensions. (See Table XV ) This part will be repeated for each set of dimensions for which the points on an I-V plot are to be obtained. The second part summarizes the outputs which are computed for each set of dimensions and gives information which will describe the output of the optimized device. (See Table XVI )

Output for a given set of dimensions.-- The values of CURDNET, VOLTAGE and ETA for the points on the I-V curve are listed in part [B]

TABLE XIV

List of Output Parameters

Fortran variable	Description
ILE	( <u>index of linear equations</u> ) A subroutine is used which solves a simultaneous system of linear equations. If ILE=0, the system is solved satisfactorily. Otherwise the system is singular to the accuracy of the computer.
PTKNT	( <u>point count</u> ) an index which is chronologically associated with a point on the I-V plot.
CURDNET	( <u>current density net</u> ) net current output per unit area of illuminated surface.
VOLTAGE	voltage output which is associated with a given value of CURDNET.
ETA	cell efficiency associated with a given pair of values of VOLTAGE and CURDNET, i.e. $ETA = CURDNET * VOLTAGE / CURDMAX / VGAP.$
VOC	( <u>open circuit voltage</u> )
VF	( <u>voltage factor</u> ) i.e. $VF = VOC / VGAP.$
CURDSC	( <u>short circuit current density</u> ) The short circuit current produced per unit area of illuminated surface.
ETACOL	( <u>collection efficiency</u> ) i.e. ETACOL $= CURDSC / CURDMAX.$
P <sub>MAX</sub> POW	( <u>maximum power point power</u> )

IMAXPOW (maximum power point current) The current per unit area of illuminated surface at the maximum power point.

VMAXPOW (maximum power point voltage)

CF (curve factor) i.e.  $CF = IMAXPOW/VOC$

CURDSC.

ETACELL (cell efficiency) i.e.  $ETACELL = IMAXPOW/POWMAX$ .

XO the thickness of the photovoltaic cell.

LN width of the n contact

LP width of the p contact

LI spacing between contacts.

H }  
K } increment sizes

CURDOPT optimum current density; the current collected per unit area of illuminated surface if every photon capable of generating a hole-electron pair is absorbed and if every optically generated hole-electron-pair is collected.

ISE (index of symmetrical equations) A subroutine is used which solves the simultaneous system of equations whose coefficient matrix must be positive definite or negative. If  $ISE=0$ , the system is solved satisfactorily. Otherwise the coefficient matrix is either singular to computer accuracy or is not positive or negative definite.

ID (index of dimensions) an index which is chronologically associated with a set of dimensions for which the points for an I-V plot are obtained.

ETAC same as ETACOL

ETACE same as ETACELL

CURDMAX (maximum current density) the current output per unit area of illuminated cell when all generated hole-electron pairs are collected.

POWMAX (maximum attainable power) the power output per unit area of illuminated surface when all the generated hole-electron pairs are collected with an output voltage equal to the energy gap voltage. I.e.  $POWMAX = CURDMAX * VGAP$ .

ETAABS (CURDMAX/CURDOPT) the ratio of the number of carriers generated in the finite thickness device to the number of carriers generated in an infinitely thick device.

TABLE XV

Printed Output for a Given Set of Dimensions

[D]	[E]	[F]		
43	1.318E+17	1.318E+17	}	
44	1.164E+17	1.162E+17		
21	9.904E+16	9.873E+16		
20	7.869E+16	7.823E+16		
25	5.249E+16	5.187E+16		
34	1.714E+16	1.640E+16		
51	5.758E+15	4.981E+15		
ILE =0				
45	3.340E+16	3.270E+16		[A]
ILE =0				
ILE =0				
54	2.480E+15	1.690E+15		
21	1.379E+15	5.823E+14		
30	1.001E+15	2.023E+14		
20	8.708E+14	7.079E+13		
20	8.251E+14	2.473E+13		

PTKNT	CURDNET	VOLTAGE	ETA	
1	0.	4.439E-01	0.	}
2	8.089E-01	4.372E-01	1.325E-01	
3	1.618E+00	4.284E-01	2.596E-01	
4	2.427E+00	4.159E-01	3.780E-01	
5	3.236E+00	3.935E-01	4.770E-01	
6	3.892E+00	3.286E-01	4.791E-01	
7	3.992E+00	2.548E-01	3.811E-01	
8	3.654E+00	3.680E-01	5.038E-01	
9	4.011E+00	1.830E-01	2.750E-01	
10	4.016E+00	1.171E-01	.762E-01	
11	4.017E+00	6.494E-02	9.774E-02	
12	4.018E+00	2.676E-02	4.028E-02	
13	4.018E+00	8.595E-04	1.294E-03	

VOC	=	.4439	}
VF	=	.6726	
CURDSC	=	4.018E+00	
ETACOL	=	.9935	
PMAXPOW	=	1.345E+00	
CMAXPOW	=	3.664E+00	
VMAXPOW	=	.3670	
CF	=	.7539	
ETACELL	=	.5038	
XO	=	5.000E-02	
LN	=	1.500E-02	
LP	=	2.500E-02	
LI	=	2.500E-03	

[C]

TABLE XVI

Summary of Outputs for Given Sets of Dimensions and Output for Optimized Device

2.570E+00	3.936E+00	4.012E+00
-8.625E-04	4.472E-04	-5.768E-06
4.472E-04	-5.112E-04	6.543E-06
-5.768E-06	6.543E-06	-5.032E-03
-6.851E-04	3.196E-04	1.189E-04
-2.063E-04	-1.167E-03	-5.032E-03
5.632E-01	8.263E-01	4.473E-04
8.263E-01	-5.632E-01	-2.187E-03
1.555E-03	-1.601E-03	1.000E+00

H = 1.000E-02 K = 2.500E-03 LI = 2.500E-03 CURDOPT = 5.000E+00 ISE = 0

ID	LN	LP	XO	VOC	VF	CURDSC	ETAC	CURDMAX	CMAXPOW	VMAXFW	FMAXPON	CF	ETACE
1	3	4	4	.4494	.6809	3.934E+00	.9964	3.948E+00	3.611E+00	.3738	1.350E+00	.7635	.5180
2	2	4	4	.4494	.6809	3.935E+00	.9967	3.5.3E+00	3.610E+00	.3738	1.350E+00	.7632	.5179
3	4	4	4	.4494	.6809	3.933E+00	.9960	3.948E+00	3.609E+00	.3737	1.348E+00	.7629	.5174
4	3	3	4	.4494	.6809	3.933E+00	.9960	3.948E+00	3.610E+00	.3738	1.349E+00	.7634	.5177
5	3	5	4	.4494	.6809	3.935E+00	.9967	3.948E+00	3.611E+00	.3738	1.350E+00	.7632	.5179
6	3	4	5	.4553	.6913	3.815E+00	.9985	3.820E+00	3.522E+00	.3818	1.345E+00	.7726	.5333
7	3	4	5	.4439	.6726	4.016E+00	.9931	4.044E+00	3.664E+00	.3671	1.345E+00	.7543	.5039
8	2	5	4	.4494	.6809	3.935E+00	.9966	3.948E+00	3.609E+00	.3737	1.349E+00	.7627	.5175
9	2	4	5	.4439	.6726	4.018E+00	.9935	4.044E+00	3.564E+00	.3671	1.345E+00	.7539	.5038
10	3	5	5	.4439	.6726	4.018E+00	.9935	4.044E+00	3.664E+00	.3670	1.345E+00	.7539	.5038

[D]

LN	=	1.285E-02
LP	=	1.968E-02
XO	=	4.012E-02
VOC	=	.4493
VF	=	.6808
CURDSC	=	3.536E+00
ETACOL	=	.9965
CURDMAX	=	3.950E+00
CMAXPOW	=	3.612E+00
VMAXPOW	=	.3738
FMAXPOW	=	1.350E+00
FORMAX	=	2.607E+00
CF	=	.7634

[E]

or Table XV. The column labeled PTKNT lists indices which are chronologically assigned to each set of values CURDNET, VOLTAGE and ETA.

In part [A] the reader will note that there are ten rows of numbers excluding the rows containing the expression,  $IIE = 0$ . Each of these rows corresponds to a row in part [B] with the first row in [A] corresponding to the first row in [B], the second row in [A] with the second row in [B], etc. The column designated by [D] gives the number of iterations required for convergence. The column designated by [E] gives the excess carrier concentrations in the middle of the n contact. The column designated by [F] gives the excess carrier concentration in the middle of the p contact.

The expressions  $IIE = 0$  result from a curve fitting routine which is used to estimate the value of CURDNET for which the maximum power will occur. (See Table XIV..)

In part [C] the output parameters and dimensions of the cell are listed.

Summary of outputs for each set of dimensions and output of optimized device.-- The cell dimensions for which output parameters have been computed and the corresponding output parameters are summarized in part [D] of Table XV. The columns headed by LN and LP list half the number of increments on the n and p contacts, and the column headed by XO lists the number of increments along the dimension of the device that is perpendicular to the illuminated surface. (The values listed under LN, LP and XO are equal to the values NLN1, NLP1 and NXO1 described on page 62 ). Note that the row of values corresponding to the number 9 in the column headed by ID is obtained from Table XV.

The list of values in part [E] of Table XVI gives the dimensions and output parameters of the optimally designed device.

The array of points shown in part [B] of Table XVI may be represented algebraically by the array shown below:

$$\begin{array}{ccc} \lambda_1 & \lambda_2 & \lambda_3 \\ v_{1ln} & v_{1lp} & v_{1xo} \\ v_{2ln} & v_{2lp} & v_{2xo} \\ v_{3ln} & v_{3lp} & v_{3xo} \end{array}$$

This array consists of the eigenvalues and orthonormal eigenvectors of the symmetric matrix with elements  $A_{ij}$ . The power may be expressed in the equation:

$$P = P_{\text{MAXPOW}} + \lambda_1 v_1^2 + \lambda_2 v_2^2 + \lambda_3 v_3^2$$

where  $v_i = v_{i ln} (n_{ln} - \bar{n}_{ln}) + v_{i lp} (n_{lp} - \bar{n}_{lp}) + v_{i xo} (n_{xo} - \bar{n}_{xo})$

for  $i = 1, 2$  and  $3$ .

Preceding page blank

```

REAL LN, LP, LI, NS INITE, NO, K, M, MDPEOK, MAGIDUM, MAGIMAX, NI, NOPPO, NSMAX
1, KTOE, AN, NP, JUNCPOI, LNJOIJ, NST2, VO2, VS4, NO4, KOZDNEH, KOZDPEH, EL(200
2), W(200), X(200), Y(200), Z(200), CRNT(100), VOLT(100), NS1(22,49), NS2(2
32,49), NS3(22,49), MAGI1(22,49), MAGI2(22,49), MAGI3(22,49), NS(22,49),
4MAGI(22,49), DJMMY(22,49), DUMAG(22,49), DNDT(22,49), NEI(22,49), CURDX
5(49), CURDY(49)
REAL NSBAR, NSSBAR, NI2, GBULK(22)
REAL NCINC, N1, N2, N3, NSRF
INTEGER R, S, RH, SH, RP1, SP1, RHP1, SHP1
INTEGER RH2
INTEGER RI, RIM1, SIP1, SI
INTEGER PATHKNT, PATHNMB
INTEGER PTKNT
REAL NLN, NLP, NXO, NLI, VOCD(50), VFD(50), CURDSCD(50), ETACOLD(50),
PMXPWD(50), CMXPWD(50), VMXPWD(50), CFD(50), ETAD(50), CURDMXD(50)
DIMENSION XM(3,1), EIGVAL(3)
DIMENSION CUMGEV(82)
COMMON IET, JLNP, JLNM, JLPP, JLPM, JXJP, JXOM, LNLP, LNXO, LPXO, RJCLN,
RTCLP, RIXO, BM(3,1), AM(3,3), JVLNT(50), JVLPL(50), JNXO(50), ID

```

LISTING OF PHYSICAL PARAMETERS

```

KT OE=0.0259
DP=48.0
DN=96.0
HI=2.5E13
PO=NI
RCOMFAC=2.8E-14
VSB=100.
VST=100.
VGAP=0.65
CURDOPT=1.

```

LISTING OF PROGRAM PARAMETERS

```

IC=2
NESHNMB=1
IH=2
LL=0
IMAX=150
ICOPMIN=20
ITVAR=1
IPATH=1
ICURVP=0
EPSILON=0.001
NCINC=5.0
RF=0.35
FACTGR=5.0

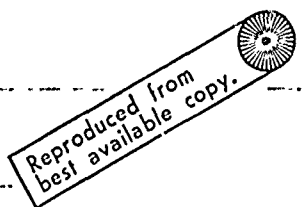
```

LISTING OF DIMENSION PARAMETERS

```

NFI=MI=6
NFI=LP=10
NFI=NXO=4
NFI=2
NFI=NL=1
NFI=1.25E-2*12.
NFI=0.25E-2

```



290  
300  
400  
500  
600  
700  
800  
830  
860  
900  
1000  
1100  
1200  
1300  
1303  
1330  
1300  
1350  
1400  
1450  
1500  
1500  
1500  
1550  
1700  
1800  
1850  
1900  
1950  
2000  
2000  
2100  
2100  
2200  
2250  
2300  
2400  
2450  
2500  
2500  
2500  
2550  
2700  
2700  
2800  
2800  
2900  
2900  
3000  
3000  
3100  
3100

LISTING OF RELAXATION FACTORS

OMEGAB=1.92  
OMEGAS=1.4  
OMEGABH = 1.92  
OMEGASB=0.9  
OMEGAST=1.4  
OMEGAC=1.4  
OMEGACH=1.4

3450  
3500  
3550  
3600  
3650  
3700  
3750  
3800  
3850  
3900  
3950

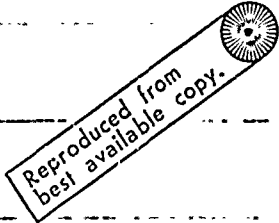
EVALUATION OF SCALE FACTOR AND READIN AND SCALING OF CUMGEN

READ(5,685) CJRDSCL  
SCALE=CURDOPT/CJRDSCL  
DO 3 NX=1,82  
READ(5,685) CJMGEN(NX)  
CUMGEN(NX)=CJMGEN(NX)\*SCALE  
GSURF=CUMGEN(2)-CUMGEN(1)

4000  
4050  
4100  
4150  
4200  
4250  
4300  
4350  
4400

LISTING OF FIXED CONSTANTS AND PRELIMINARY COMPUTATIONS

DU=LMAX-LH  
ALPHA=2.0\*DN\*DP/(DN+DP)  
PC=NI\*NI/PC  
NOPPO=NC+PO  
POPNO=PC+NO  
PC2=PC+PC  
PO2=PO+PO  
PC4=PO2+PO2  
PC2=NO+NO  
NO4=NO2+NO2  
ECC=(PC+NC)/2.  
LCC=(DP\*PO+DN\*NO)/(DP+DN)  
L2=NI+NI  
D=0  
IT=IC  
LPTS=0  
LXXOM=3



4450  
4500  
4550  
4600  
4650  
4700  
4750  
4800  
4850  
4900  
4950  
5000  
5050  
5100  
5150  
5200  
5250  
5300  
5350  
5400

BEGIN LOOP FOR EVALUATION OF POINTS ON I-V CURVE

D=D+1  
LN=NLN1  
LNP=NLP1  
YD=NXO1  
INITL=NLN1+NLP1+NL11  
INITL=NXO1  
LN=LN\*K\*2.0  
LNP=LNP\*K\*2.0  
LNL=LNL\*K  
LNXO=H  
LXNET=0.0  
LH=H/12.5E-4+0.5  
LGEN=CUMGEN(LXO1\*NLH+2)-CUMGEN(L)  
LNL=1  
LXNET=L  
LXNETMAX=(GSURF+BULKGEN)\*1.6e-19  
LXNETMAX=CURDMAX\*VGAP  
LX=(LNP+L)/2.0+L1  
LXODS=ALPHA\*LPTS\*LXNET/(LXO1\*LXO1+YD\*YD)

5450  
5500  
5550  
5600  
5650  
5700  
5750  
5800  
5850  
5900  
5950  
6000  
6050  
6100  
6150  
6200  
6250  
6300  
6350  
6400  
6450  
6500

C	LISTING OF TERMS THAT MUST BE RESET FOR NEW VALUES OF CURDNET	75
C		77
C		78
C	10 I=IINITL	79
C	J=JINITL	80
C	MESHKNT=1	81
C		83
C	VALJE OF INDXITL SET TO CAUSE INITIALIZATION	85
C		87
C	INDXITL=0	89
C		91
C	EVALUATE I AND J DEPENDENT TERMS	92
C		93
C	COMPUTATION OF INCREMENT SIZES	94
C		95
C	30 REALI=I	96
C	H=XO/REALI	97
C	REALJ=J	98
C	K=((LN+LP)/2.+LI)/REALJ	99
C		100
C	COMPUTATION OF INCREMENT DEPENDENT VARIABLES	101
C		102
C	AK=ALPHA/(K*K)	103
C	AH=ALPHA/(H*H)	104
C	HO2DNE=H/2.0/DN/1.6E-19	105
C	HO2DPE=H/2.0/DP/1.6E-19	106
C	MDPEOK=-DP*1.6E-19/K	107
C	H2=2.0*H	108
C	DNEOK=DN*1.6E-19/K	109
C	AH2PAK2=2.0*AH+2.0*AK	110
C	P2=2.0*RCOMFAC	111
C	HSOKS=H*H/K/K	112
C	HSOKSP1=HSOKS+1.0	113
C	HOATGS=H/ALPHA*GSURF	114
C	DP2EKOH=DP*2.0*1.60E-19*K/H	117
C	DN2EKOH=DN*2.0*1.6E-19*K/H	118
C	KO2DNEH=K/2.0/DN/1.6E-19/H	119
C	KO2DPEH=K/2.0/DP/1.6E-19/H	120
C	HO2DNEK=H/2.0/DN/1.6E-19/K	121
C	HC2DPEK=H/2.0/DP/1.6E-19/K	122
C	HVSTO2A=H*VST/2.0/ALPHA	123
C	HVSBO2A=H*VSB/2.0/ALPHA	124
C		121
C	LISTING OF ITERATION INDICES	122
C		123
C	RH=(LN/(2.*K)+0.5	124
C	SH=(LN/2.+LI)/K+1.5	125
C	S=SH	126
C	RHP1=RH+1	127
C	R=RHP1	128
C	SHP1=SH+1	129
C	RPI=R+1	130
C	SPI=S+1	131
C	JH=J+1	132
C	JN=J+2	133
C	IH=I+2	134
C	IN=IH	135
C	JHM=JH-1	136
C	JNM=JN-1	137
C	INM=IN-1	138
C	IHM=IH-1	139

LISTING OF TERMS DEPENDENT ON ITERATION INDICES

SMR=S-R  
 RJNM2=JN-2  
 TERM1=N1+(VST+VSB\*SMR/RJNM2)/R2/XD  
 TERM2=VST/R2/XD/RJNM2  
 TERM3=VSB/R2/XD/RJNM2  
 BULKPTS=(IN-2)\*(JN-2)

EVALUATION OF GBULK

ICJ=I\*NIH+2  
 DO 35 NX=2, INM1  
 ICL=ICJ-NIH  
 GBULK(NX)=(CJMGEN(ICJ)-CJMGEN(ICL))/H  
 ICJ=ICL

LISTING OF TESTPOINT INDICES

INDXXC=(IN+2)/2  
 INDXYC=(JN+2)/2  
 INDXXF=IV-1  
 INDXXN=R  
 INDXXPN=SP1



LISTING OF TERMS THAT MUST CHANGE WITH EACH NEW VALUE OF CURDNET

GBADXR=(GSJRF+BJLKGFN-CJRDNET/1.6E-19)/XD/RCQMFAC  
 NSINITL=-TERM1\*SQRT(TERM1\*TERM1+GBADXR)

INITIALIZATION OF MAGI AND NS

IF(INDXILL.NE.O) GO TO 45  
 INDXIFL=1  
 IP2=I+2  
 JP2=J+2  
 DO 20 NX=1,IP2  
 DO 20 NY=1,JP2  
 MAGI(NX,NY)=0.0  
 20 NS(NX,NY)=NSINITL  
 NSMAX=FACTOR\*(1+V\*SQRT(VI\*VI+GBADXR))

BOUNDARY CONDITIONS ON MAGI ON THE BACK SURFACE WITH N COORDINATES

40 MAGIMAX=CIPMHI\*ALPHA\*(V/2.04E11)  
 DO 50 NY=REP1,SP1  
 50 MAGI(2,NY)=MAGIMAX  
 DELTALB=OMEGA/2\*(1+2PAK2+2PAK(VSMAX+AF1))  
 DELTALC=OMEGA/VEGAC\*DELTA

RESET LOOPKNT = 0

LOOPKNT=0

PRINT F, E, M, C, S, P, A, D, S, N, A, S

60 IF (LOOPKNT.EQ.1) GOTO 10  
 2000 IF (NSMAX.GT.1.0) GOTO 2000  
 2010 IF (NSMAX.GT.1.0) GOTO 2000  
 2020 IF (NSMAX.GT.1.0) GOTO 2000  
 2030 IF (NSMAX.GT.1.0) GOTO 2000

14000  
 14001  
 14002  
 14003  
 14004  
 14005  
 14006  
 14007  
 14008  
 14009  
 14010  
 14011  
 14012  
 14013  
 14014  
 14015  
 14016  
 14017  
 14018  
 14019  
 14020  
 14021  
 14022  
 14023  
 14024  
 14025  
 14026  
 14027  
 14028  
 14029  
 14030  
 14031  
 14032  
 14033  
 14034  
 14035  
 14036  
 14037  
 14038  
 14039  
 14040  
 14041  
 14042  
 14043  
 14044  
 14045  
 14046  
 14047  
 14048  
 14049  
 14050  
 14051  
 14052  
 14053  
 14054  
 14055  
 14056  
 14057  
 14058  
 14059  
 14060  
 14061  
 14062  
 14063  
 14064  
 14065  
 14066  
 14067  
 14068  
 14069  
 14070  
 14071  
 14072  
 14073  
 14074  
 14075  
 14076  
 14077  
 14078  
 14079  
 14080  
 14081  
 14082  
 14083  
 14084  
 14085  
 14086  
 14087  
 14088  
 14089  
 14090  
 14091  
 14092  
 14093  
 14094  
 14095  
 14096  
 14097  
 14098  
 14099  
 14100

```

10 WRITE (6,550) (NS/NX,NY),NY=1,JN)
   WRITE (6,560)
   DO 80 NX=2,IH
80  WRITE (6,550) (MAGI(NX,NY),NY=1,JH)
   WRITE (6,560)
   IF ((LOOPKNT.GE.LMAX).AND.(INDXETA.EQ.1)) GO TO 228
90  IF (LOOPKNT.GE.LMAX) GO TO 515
   LOOPKNT=LCOPKNT+1
C
C P CONTACT--APPROXIMATION OF MAGI AND VS, AND EVALUATION OF W AND Y
C
   IF (SP1.EQ.JNM1) NS(1,SP1)=VS(2,SP1)
1+H02DPEK*(MAGI(2,SHP1)-MAGI(2,SH))
   IF (SP1.EQ.JNM1) GO TO 115
   W(SH)=0.0
   Y(SP1)=1.0
   DO 100 NY=SHP1,JHMI
   NST2=NS(2,NY)+NS(1,NY)
   GP=DP2EKOH*(NST2+POPNO)/(NST2+ND2)
   NS4=NS(2,NY+1)+NS(2,NY)+NS(1,NY+1)+NS(1,NY)
   GN=KO2DNEH*(NS4+PO4)/(NS4+PO2PND2)
   MAGI(2,NY)=MAGI(2,NY-1)-GP*(VS(2,NY)-VS(1,NY))
   W(NY)=W(NY-1)+GP*Y(NY)
   NS(1,NY+1)=NS(1,NY)-GN*(3.0*(MAGI(3,NY)-MAGI(2,NY))-(MAGI(4,NY)-MAGI(3,NY)))
   Y(NY+1)=Y(NY)+(GN+GN+GN)*W(NY)
100
C
C P CONTACT--EVALUATION OF DELTA
C
   NST2=NS(2,JNM1)+NS(1,JNM1)
   GP=DP2EKOH*(NST2+POPNO)/(NST2+ND2)
   DELTA=(MAGI(2,JH)-MAGI(2,JHMI)+GP*(NS(2,JNM1)-NS(1,JNM1)))/(W(JHMI)
1+GP*Y(JNM1))
C
C P CONTACT--EVALUATION OF MAGI AND VS
C
   DO 110 NY=SHP1,JHMI
   MAGI(2,NY)=MAGI(2,NY)+W(NY)*DELTA
110 NS(1,NY)=NS(1,NY)+Y(NY)*DELTA
   NS(1,JNM1)=NS(1,JNM1)+Y(JNM1)*DELTA
C
C NC CONTACT--APPROXIMATION OF MAGI AND VS, AND EVALUATION OF W AND Y
C
115 IF (R.EQ.2) NS(1,2)=NS(2,2)-KO2DNEK*(MAGI(2,2)-MAGI(1,2))
   IF (R.EQ.2) GO TO 135
   W(1)=0.0
   Y(2)=1.0
   DO 120 NY=2,3H
   NST2=NS(2,NY)+NS(1,NY)
   GN=DN2EKOH*(NST2+POPNO)/(NST2+PD2)
   NS4=NS(2,NY+1)+NS(2,NY)+NS(1,NY+1)+NS(1,NY)
   GP=KO2DPEH*(NS4+PO4)/(NS4+PO2PND2)
   MAGI(2,NY)=MAGI(2,NY-1)+GN*(NS(2,NY)-NS(1,NY))
   W(NY)=W(NY-1)-GN*Y(NY)
   NS(1,NY+1)=NS(1,NY)+GN*(3.0*(MAGI(3,NY)-MAGI(2,NY))-(MAGI(4,NY)-MAGI(3,NY)))
   Y(NY+1)=Y(NY)+(GN+GN+GN)*W(NY)
120
C
C N CONTACT--EVALUATION OF DELTA
C
   NST2=NS(2,R)+NS(1,R)

```

Reproduced from  
best available copy.

174  
175  
176  
177  
178  
179  
180  
181  
182  
183  
184  
185  
186  
187  
188  
189  
189  
189  
190  
191  
192  
193  
194  
195  
196  
197  
198  
199  
200  
201  
202  
203  
204  
205  
206  
207  
208  
209  
210  
211  
212  
213  
214  
215  
216  
217  
218  
219  
220  
221  
222  
223  
224  
225  
226  
227  
228  
229  
230  
231  
232  
233  
234  
235  
236  
237  
238  
239  
240  
241  
242  
243  
244  
245  
246  
247  
248  
249  
250  
251  
252  
253  
254  
255  
256  
257  
258  
259  
260  
261  
262  
263  
264  
265  
266  
267  
268  
269  
270  
271  
272  
273  
274  
275  
276  
277  
278  
279  
280  
281  
282  
283  
284  
285  
286  
287  
288  
289  
290  
291  
292  
293  
294  
295  
296  
297  
298  
299  
300  
301  
302  
303  
304  
305  
306  
307  
308  
309  
310  
311  
312  
313  
314  
315  
316  
317  
318  
319  
320  
321  
322  
323  
324  
325  
326  
327  
328  
329  
330  
331  
332  
333  
334  
335  
336  
337  
338  
339  
340  
341  
342  
343  
344  
345  
346  
347  
348  
349  
350  
351  
352  
353  
354  
355  
356  
357  
358  
359  
360  
361  
362  
363  
364  
365  
366  
367  
368  
369  
370  
371  
372  
373  
374  
375  
376  
377  
378  
379  
380  
381  
382  
383  
384  
385  
386  
387  
388  
389  
390  
391  
392  
393  
394  
395  
396  
397  
398  
399  
400

DN=DN2EKOH\*(NST2+POPNO)/(NST2+PJ2)  
 DELTA=(MAGI(2,RHP1)-MAGI(2,RH)-GN\*(VS(2,R)-NS(1,R)))/(W(RH)-GN\*Y(R  
 1))

N CONTACT--EVALUATION OF MAGI AND NS

DO 130 NY=2, RH  
 MAGI(2, NY)=MAGI(2, NY)+W(NY)\*DELTA  
 130 NS(1, NY)=NS(1, NY)+Y(NY)\*DELTA  
 NS(1, R)=NS(1, R)+Y(R)\*DELTA

NS IN INTERIOR REGION

15 DELTAT=DELTATC  
 DO 150 NX=2, INM1  
 DO 140 NY=2, JNM1  
 DNDET(NX, NY)=AH\*(NS(NX+1, NY)-NS(NX, NY)-NS(NX, NY)+NS(NY-1, NY))+AK\*(N  
 IS(NX, NY+1)-NS(NX, NY)-NS(NX, NY)+NS(NX, NY-1))+GBULK(NX)-RCDFAC\*NS(N  
 2X, NY)\*(NS(NX, NY)+NOPPO)  
 NS(NX, NY)=NS(NX, NY)+DNDET(NX, NY)\*DELTAT  
 IF (NS(NX, NY).LT.1.0) NS(NX, NY)=1.0  
 140 IF (NS(NX, NY).GE.NSMAX) NS(NX, NY)=NSMAX  
 150 DELTAT=DELTATB

EVALUATION OF NEI

DO 160 NX=2, INM1  
 DO 150 NY=2, JNM1  
 160 NEI(NX, NY)=1.0/(NS(NX, NY)+ACCC)

MAGI IN INTERIOR REGION

OMEGAH=OMEGACH  
 DO 170 NX=3, IHM1  
 NXPI=NX+1  
 NXMI=NX-1  
 DO 170 NY=2, JHM1  
 NYPI=NY+1  
 MAGI(IJM)=(NEI(NX, NYPI)+NEI(NX, NY))\*MAGI(NXPI, NY)+(NEI(NXMI, NYPI)+N  
 1EI(NXMI, NY))\*MAGI(NYMI, NY)+HSOKS\*((NEI(NX, NYPI)+NEI(NXPI, NYPI))+MA  
 2GI(NX, NYPI)+(NEI(NX, NY)+NEI(NXMI, NY))\*MAGI(NX, NY-1))/(HSOKSPI\*(NE  
 3I(NX, NYPI)+NEI(NXMI, NYPI)+NEI(NX, NY)+NEI(NXMI, NY))  
 MAGI(NX, NY)=MAGI(NX, NY)+OMEGAH\*(MAGI(NX, NY)-MAGI(NX, NY))  
 170 OMEGAH=OMEGASABH

NS AT TOP SURFACE

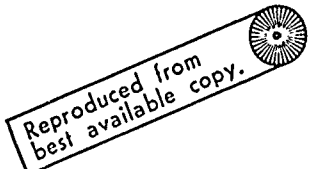
DO 180 NY=2, JNM1  
 M=NS(INM1, NY)+HJATGS-HVSTDPAA\*(NS(INM1, NY)+NS(1, NY))  
 180 NS(IN, NY)=NS(IN, NY)+OMEGASABH\*(M-NS(IN, NY))

NS AT BOTTOM SURFACE

IF (RPI.GE.5) GO TO 200  
 DO 190 NY=2, JNM1  
 M=NS(1, NY)+HJATGS-HVSTDPAA\*(NS(1, NY)+NS(INM1, NY))  
 190 NS(1, NY)=NS(1, NY)+OMEGASABH\*(M-NS(1, NY))

NS AT LEFT SIDE

DO 210 NX=2, INM1





50	PATHNMB=R-1	34100
	KN=R	34200
	KP=SP1	34300
	KX=2	34400
	DO 310 PATHKNT=1, PATHNMB	34500
		34600
	EVALUATION OF EXCESS CARRIER CONCENTRATIONS AT JUNCTIONS	34700
		34800
	NN=(NS(2,KN)+NS(1,KN))/2.0	34900
	NP=(NS(2,KP)+NS(1,KP))/2.0	35000
	IF(IPATH.EQ.1) GO TO 255	35050
	WRITE(6,580) MESHKNT, PATHKNT	35100
	WRITE(6,550) NN, NP	35200
	CONTINJE	35230
	IF(KN.EQ.2) WRITE(6,610) LDDPKNT, NN, NP	35260
	IF((NN.GT.0.0).AND.(NP.GT.0.0)) GO TO 260	35300
	IF((MESHKNT.EQ.MESHNMB).AND.(KN.EQ.2)) GO TO 515	35400
	GO TO 300	35500
		35600
	INITIAL POINTS IN THE GRAPHICAL INTEGRAL ALONG THE X AXIS	35700
		35800
250	PTNE=(NN+NS(2,KN))/2.0+ACCC	35900
	PTDHDY=(3.0*(MAGI(2,KN)-MAGI(2,KN-1))/K+(MAGI(3,KN)-MAGI(3,KN-1))/	36000
	IK)/4.0	36100
	GIXN=PTDHDY/PTNE*H/2.0	36200
	PTNE=(NP+NS(2,KP))/2.0+ACCC	36300
	PTDHDY=(3.0*(MAGI(2,KP)-MAGI(2,KP-1))/K+(MAGI(3,KP)-MAGI(3,KP-1))/	36400
	IK)/4.0	36500
	GIXP=PTDHDY/PTNE*H/2.0	36500
		36700
	EVALUATION OF GRAPHICAL INTEGRALS ALONG THE X AXIS	36800
		36900
	IF(KX.LT.3) GO TO 280	37000
	DO 270 NX=3, KX	37100
	PTNE=(NS(NX-1,KN)+NS(NX,KN))/2.0+ACCC	37200
	PTDHDY=(MAGI(NX,KN)-MAGI(NX,KN-1))/K	37300
	GIXN=GIXN+PTDHDY/PTNE*H	37400
	PTNE=(NS(NX-1,KP)+NS(NX,KP))/2.0+ACCC	37500
	PTDHDY=(MAGI(NX,KP)-MAGI(NX,KP-1))/K	37500
270	GIXP=GIXP+PTDHDY/PTNE*H	37700
		37900
	EVALUATION OF GRAPHICAL INTEGRAL ALONG THE Y AXIS	37900
		38000
200	KPM1=KP-1	38100
	GIY=0.0	38200
	DO 290 NY=KN, KPM1	38300
	PTNE=(NS(KX,NY)+NS(KX,NY+1))/2.0+ACCC	38400
	PTDHDY=(MAGI(KX+1,NY)-MAGI(KX,NY))/H	38500
290	GIY=GIY+PTDHDY/PTNE*K	38500
		38700
	EVALUATION OF OUTPUT VOLTAGE, POWER AND EFFICIENCY	38800
		38900
	OHMLOSS=KTOE/1.6E-19/(DN+DP)*(GIXN-GIY-GIXP)	39000
	DIFFPOT=KTOE*(DN-DP)/(DN+DP)*ALOG((NP+ACCC)/(NN+ACCC))	39100
	JUNCPOT=KTOE*ALOG((NN+NO)*(NP+PO)/NI/NI)	39200
	VOLTAGE=JUNCPOT+DIFFPOT-OHMLOSS	39300
	POWER=VOLTAGE*CJRDNET	39400
	ETA=POWER/POJMAX	39500
	ETACJRD=CJRDNET/CJRDMAX	39500
	ETAJ=VOLTAGE/VGAP	39700
		39800

WRITEOUT OF VALUES RELATED TO CURDNET, VOLTAGE AND POWER	3990
	4000
IF (IPATH.EQ.1) GO TO 300	4005
WRITE (6,550) CJRDNET,VOLTAGE,JUNCPOT,DIFFPOT,OHMLOSS	4010
WRITE (6,550) POWER,POWMAX,ETA,ETACURD,ETA V	4020
	4030
RESET OF PATH OF INTEGRATION	4040
	4050
310 KN=KN-1	4050
IF (PATHNMB.EQ.1) GO TO 310	4070
KP=SPI+(JNMI-SPI)*(PATHKNT)/(PATHNMB-1)	4080
KX=2+(INMI-2)*(PATHKNT)/(PATHNMB-1)	4090
310 CONTINUE	4100
	4120
START A NEW MESH UNLESS THE FINEST MESH HAS JUST BEEN COMPLETED	4130
	4140
IF (MESHKNT.NE.MESHNMB) GO TO 450	4150
	4160
BEGIN STORAGE AND INTERPOLATION WITH PROCEEDURE FOR FIRST ITERATION	4170
	4180
IF (PTKNT.NE.1) GO TO 340	4190
DO 320 NX=1,IN	4200
DO 320 NY=1,JN	4210
320 NS2(NX,NY)=NS(NX,NY)	4220
DO 330 NX=2,IHM1	4230
DO 330 NY=2,JHM1	4240
330 MAGI2(NX,NY)=MAGI(NX,NY)	4250
V2=VOLTAGE	4250
VOLI(1)=V2	4270
C2=CJRDNET	4280
CRNT(1)=C2	4290
PTKNT=2	4300
	4300
EVALUATION OF CURRENT AND VOLTAGE INCREMENTS	4300
	4300
CINCREG=CJRDMAX/NCINC	4300
CJRDINC=CINCREG	4300
CURDNET=CJRDNET+CJRDINC	4310
GO TO 10	4320
	4330
INTERPOLATION PROCEEDURE FOR SECOND ITERATION	4340
	4350
IF (PTKNT.NE.2) GO TO 390	4350
DO 350 NX=1,IN	4370
DO 350 NY=1,JN	4380
350 NS1(NX,NY)=NS(NX,NY)	4390
DO 360 NX=2,IHM1	4400
DO 360 NY=2,JHM1	4410
360 MAGI1(NX,NY)=MAGI(NX,NY)	4420
V1=VOLTAGE	4430
VOLI(2)=V1	4440
C1=CJRDNET	4450
CRNT(2)=C1	4460
PTKNT=3	4470
CURDNET=CJRDNET+CJRDINC	4480
DO 370 NX=1,IN	4490
DO 370 NY=1,JN	4500
370 NS(NX,NY)=NS1(NX,NY)+NS2(NX,NY)-NS2(NX,NY)	4510
DO 380 NX=2,IHM1	4520
DO 380 NY=2,JHM1	4530
380 MAGI(NX,NY)=MAGI1(NX,NY)+MAGI2(NX,NY)-MAGI2(NX,NY)	4540

GO TO 440

45500

BEGIN QUADRATIC INTERPOLATIONS WITH INITIALIZATIONS

45600

45700

45800

45900

46000

46100

46200

46300

46400

46500

46600

46700

46800

46900

47000

47100

47200

47300

47400

47500

47600

47700

47800

47920

47940

47950

47960

47980

47990

48001

48020

48040

48060

48080

48100

48200

48300

48450

48550

48650

48700

48750

48800

48850

48900

48950

49000

49050

49100

49200

49240

49290

49340

49390

49440

49470

49500

49530

49540

COMPUTATION OF MATRIX ELEMENTS

D11=-1.0/(C3-C1)/(C1-C2)

D12=-1.0/(C1-C2)/(C2-C3)

D13=-1.0/(C2-C3)/(C3-C1)

D21=(C2+C3)/(C3-C1)/(C1-C2)

D22=(C3+C1)/(C1-C2)/(C2-C3)

D23=(C1+C2)/(C2-C3)/(C3-C1)

D31=-C2\*C3/(C3-C1)/(C1-C2)

D32=-C3\*C1/(C1-C2)/(C2-C3)

D33=-C1\*C2/(C2-C3)/(C3-C1)

EVALUATION OF VOLTAGE COEFFICIENTS

AV=D11\*V1+D12\*V2+D13\*V3

BV=D21\*V1+D22\*V2+D23\*V3

CV=D31\*V1+D32\*V2+D33\*V3

IF ((AMINI(V1,V2,V3).LT.KTOE).AND.(INDXETA.EQ.4)) GO TO 520

IF ((NN.LT.NI).OR.(NP.LT.NI)) GO TO 520

REFINED ESTIMATE OF MAXIMUM POWER POINT

IF (INDXETA.NE.3) GO TO 395

INDXETA=4

CALL CRVFIT(CRNT,VOLT,PTKNT,INDXETA,CMAXPOW,PMAXPOW)

CMAXPOW=PMAXPOW/CMAXPOW

TEST FOR ETAMAX

IF (INDXETA.EQ.2) GO TO 396

IF ((ETA.GT.ETA1).OR.(INDXETA.NE.1)) GO TO 397

INDXETA=INDXETA+1

CALL CRVFIT(CRNT,VOLT,PTKNT,INDXETA,CURDNET,PMAXPOW)

DIFMIN=AMINI(ABS(C1-CURDNET),ABS(C2-CURDNET))

RATIO=DIFMIN/CURDNET

IF (RATIO.LT.0.003) GO TO 394

IF (IITVAR.EQ.1) GO TO 410

WRITE (6,590)

GO TO 410

COMPUTATION OF CURDNET

CURDNET=AMAX1(C1,C2,C3)+CINCRFG

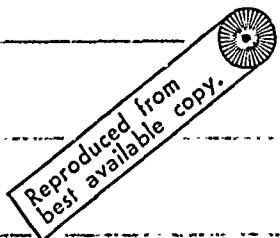
JNM3=IN-3

DO 399 NY=2,JNM1,JNM3

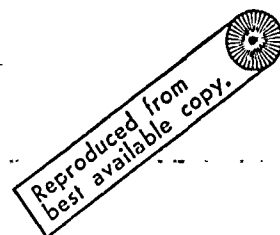
Q=NS(2,NY)+NS(1,NY)

RP=NS1(2,NY)+NS1(1,NY)

RB=NS2(2,NY)+NS2(1,NY)



	F11=-1.0/(N3-N1)/(N1-N2)	4969
	F12=-1.0/(N1-N2)/(N2-N3)	4974
	F13=-1.0/(N2-N3)/(N3-N1)	4979
	F21=-(N2+N3)*F11	4984
	F22=-(N3+N1)*F12	4989
	F23=-(N1+N2)*F13	4994
	F31=N2*N3*F11	4999
	F32=N3*N1*F12	5004
	F33=N1*N2*F13	5009
	A=F11*C1+F12*C2+F13*C3	5014
	B=F21*C1+F22*C2+F23*C3	5019
	C=F31*C1+F32*C2+F33*C3	5024
	NSRF=AMIN1(N1,N2,N3)*RF	5029
	CURDTRY=A*NSRF*NSRF+B*NSRF+C	5034
399	CURDNET=AMIN1(CJRDNET,CURDTRY)	5037
C		5040
C	INTERPOLATION FOR NS	5050
C		5060
410	CURDNTS=CJRDNET*CURDNET	5075
	DO 420 NX=1, IN	5090
	DO 420 NY=1, JN	5100
	NS3(NX, NY)=NS2(NX, NY)	5110
	NS2(NX, NY)=NS1(NX, NY)	5120
	NS1(NX, NY)=NS(NX, NY)	5130
	A=D11*NS1(NX, NY)+D12*NS2(NX, NY)+D13*NS3(NX, NY)	5140
	B=D21*NS1(NX, NY)+D22*NS2(NX, NY)+D23*NS3(NX, NY)	5150
	C=D31*NS1(NX, NY)+D32*NS2(NX, NY)+D33*NS3(NX, NY)	5160
420	NS(NX, NY)=A*CJRDNTS+B*CURDNET+C	5170
C		5180
C	INTERPOLATION FOR MAGI	5190
C		5200
	DO 430 NX=2, IHMI	5210
	DO 430 NY=2, JHMI	5220
	MAGI3(NX, NY)=MAGI2(NX, NY)	5230
	MAGI2(NX, NY)=MAGI1(NX, NY)	5240
	MAGI1(NX, NY)=MAGI(NX, NY)	5250
	A=D11*MAGI1(NX, NY)+D12*MAGI2(NX, NY)+D13*MAGI3(NX, NY)	5260
	B=D21*MAGI1(NX, NY)+D22*MAGI2(NX, NY)+D23*MAGI3(NX, NY)	5270
	C=D31*MAGI1(NX, NY)+D32*MAGI2(NX, NY)+D33*MAGI3(NX, NY)	5280
430	MAGI(NX, NY)=A*CJRDNTS+B*CURDNET+C	5290
	PTKNT=PTKNT+1	5300
440	ETAL=ETA	5310
	GO TO 40	5320
C		5330
C	CHECK AND INCREMENT MESHKNT	5340
C		5350
450	MESHKNT=MESHKNT+1	5360
C		5370
C	BEGIN REMESHING BY STORING NS IN DUMMY AND MAGI IN DUMAG	5380
C		5390
	IX=1	5400
	DO 470 NX=1, IN	5410
	IY=1	5420
	DO 460 NY=1, JN	5430
	DUMMY(IX, IY)=NS(NX, NY)	5440
	DUMAG(IX, IY)=MAGI(NX, NY)	5450
460	IY=IY+1	5460
470	IX=IX+1	5470
C		5480
C	COMPUTE DUMMY AND DUMAG AT HORIZONTAL INTERMEDIATE POINTS	5490
C		5500



```

IXMAX=3*INM1+1
ILEFTMX=3*JN-5
DO 480 IX=1, IXMAX, 3
DO 480 ILEFT=1, ILEFTMX, 3
IRIGHT=ILEFT+3
DUMMY(IX, ILEFT+1)=(DJMMY(IX, ILEFT)+DUMMY(IX, ILEFT)+DUMMY(IX, IRIGHT))/3.0
DJMAG(IX, ILEFT+1)=(DJMAG(IX, ILEFT)+DUMAG(IX, ILEFT)+DUMAG(IX, IRIGHT))/3.0
DUMMY(IX, ILEFT+2)=(DJMMY(IX, ILEFT)+DUMMY(IX, IRIGHT)+DUMMY(IX, IRIGHT))/3.0
DJMAG(IX, ILEFT+2)=(DJMAG(IX, ILEFT)+DUMAG(IX, IRIGHT)+DUMAG(IX, IRIGHT))/3.0

COMPUTE DJMMY AND DJMAG AT VERTICAL INTERMEDIATE POINTS

ILOWMAX=3*IN-5
IYMAX=3*JNMI+1
DO 490 ILOW=1, ILOWMAX, 3
DO 490 IY=1, IYMAX
IHIGH=ILOW+3
DUMMY(ILOW+1, IY)=(DJMMY(ILOW, IY)+DUMMY(ILOW, IY)+DUMMY(IHIGH, IY))/3.0
DUMMY(ILOW+2, IY)=(DUMMY(ILOW, IY)+DUMMY(IHIGH, IY)+DUMMY(IHIGH, IY))/3.0
DJMAG(ILOW+1, IY)=(DJMAG(ILOW, IY)+DUMAG(ILOW, IY)+DUMAG(IHIGH, IY))/3.0
DJMAG(ILOW+2, IY)=(DUMAG(ILOW, IY)+DUMAG(IHIGH, IY)+DUMAG(IHIGH, IY))/3.0

TRANSFER DJMMY INTO NEW NS MESH

IN=3*IN-4
JN=3*JN-4
DO 500 NX=1, IN
DO 500 NY=1, JN
NS(NX, NY)=DJMMY(NX+1, NY+1)

TRANSFER DJMAG INTO NEW MAGI MESH

IH=3*IH-4
DO 510 NX=1, IH
DO 510 NY=1, JN
MAGI(NX, NY)=DJMAG(NX+2, NY)

RESET I AND J TO THE NUMBER OF INCREMENTS IN THE NEW MESH

I=I+I
J=J+J

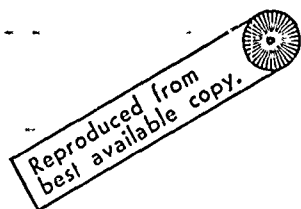
BEGIN NEW MESH

GO TO 30

SUMMARY WRITFOOT OF VOLTAGE, CURRENT AND EFFICIENCY

PI=PI-PIKAT-1
WRITE (6, 600)
DO 520 INDX=1, PIKAT
VOLTMP=VOLT(INDX)
COTMP=CRAT(INDX)

```



55100  
55200  
55300  
55400  
55500  
55600  
55700  
55800  
55900  
56000  
56100  
56200  
56300  
56400  
56500  
56600  
56700  
56800  
56900  
57000  
57100  
57200  
57300  
57400  
57500  
57600  
57700  
57800  
57900  
58000  
58100  
58200  
58300  
58400  
58500  
58600  
58700  
58800  
58900  
59000  
59100  
59200  
59300  
59400  
59500  
59600  
59700  
59800  
59900  
60000  
60100  
60200  
60300  
60400  
60500  
60600  
60700  
60800  
60900  
61000  
61100  
61200  
61300

```

ETA=CJRDTMP*VOLTTMP/POWMAX
IF(ICJRVE.EQ.1) GO TO 530
WRITE (6,610) INDX,CURDTMP,VOLTTMP,ETA
CONTINUE

```

61400  
61460  
61540  
61600  
61700  
61800  
61900  
62000  
62100  
62200  
62300  
62400  
62500  
62500  
62700  
62800  
62900  
63000  
63100  
63200

SUMMARY OF OUTPUT RESULTS

```

VOC = VOLT(1)
VF=VOC/VGAP
CURDSC=(-BV-SCRT(BV*BV-4.0*AV*CV))/2.0/AV
ETACOL=CJRDC/CJRDMAX
CF=PMAXPOW/VOC/CJRDC
ETACELL=PMAXPOW/POWMAX
WRITE(6,620) VOC,VF,CURDSC,ETACOL,PMAXPOW,CMAXPOW,VMAXPOW,CF,
ETACELL,XO,LN,LP,LI,ENR
FORMAT(/,1X,5HVOC = ,F6.4/,1X,5HVF = ,F6.4/,1X,9HCURDSC = ,
E10.3/,1X,9HETACOL = ,F6.4/,1X,10HPMAXPOW = ,E10.3/,
1X,10HCMAXPOW = ,E10.3/,1X,10HVMAXPOW = ,F6.4/,1X,5HCF = ,
F6.4/,1X,10HETACELL = ,F6.4/,1X,5HXO = ,E10.3/,1X,5HLN = ,E10.3
/,1X,5HLP = ,E10.3/,1X,5HLI = ,E10.3/,1X,6HENR = ,E10.3)

```

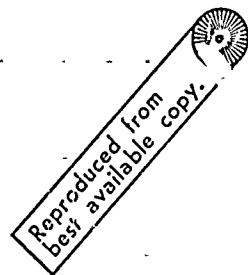
63300  
63400  
63500  
63500  
63700  
63800  
63900  
64000  
64100  
64200  
64300  
64400  
64500  
64600  
64700  
64800  
64900  
65000

STORE OUTPUTS IN VECTORS

```

VOC(D)=VOC
VFD(D)=VF
CURDSC(D)=CJRDC
CURDMXD(D)=CJRDMAX
ETACOLD(D)=ETACOL
PMAXPOW(D)=PMAXPOW
CMAXPOW(D)=CMAXPOW
VMAXPOW(D)=VMAXPOW
CF(D)=CF
ETACELL(D)=ETACELL
NLN(D)=NLN
NLP(D)=NLP
NXO(D)=NXO
IF(13PTS.EQ.1) GO TO 730

```



SELECT NEW MESH PARAMETERS

```

IF(IC.EQ.1) NLN1=NLN-1
IF(IC.EQ.2) NLN1=NLN+1
IF(IC.EQ.3) NLP1=NLP-1
IF(IC.EQ.4) NLP1=NLP+1
IF(IC.EQ.5) NXO1=NXO-1
IF(IC.EQ.6) NXO1=NXO+1

```

65100  
65200  
65300  
65400  
65500  
65600  
65700  
65800  
65900

HAVE OUTPUTS BEEN EVALUATED FOR NEW MESH PARAMETERS

```

IEL=IEVAL(NLN1,NLP1,NXO1)
IF(IEL.EQ.0) GO TO 5

```

66000  
66100  
66200  
66300  
66400

IS POWER OUTPUT FOR NEXT MESH GREATER THAN MAXIMUM POWER OUTPUT FROM PREVIOUS MESHES

```

IF(1) THEN GO TO 720
IF(VMAXPOW(1) > PMAXPOW(1)) GO TO 720
IF(NLN1 > NLN) THEN GO TO 720
IF(NLP1 > NLP) THEN GO TO 720
IF(NXO1 > NXO) THEN GO TO 720
IF(1) THEN
NLP1=NLN1

```

66500  
66600  
66700  
66800  
66900  
67000  
67100

NXOT=NXOI  
IDXXOM=3  
IT=IC  
I3PTS=0  
GO TO 700

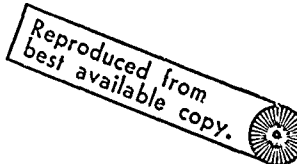
67200  
67300  
67400  
67500  
67600  
67700  
67800  
67900

HAS THE POWER OUTPUT BEEN EVALUATED FOR THE SIX MESH  
ARRANGEMENTS ADJASCENT TO THE MESH MAXIMUM POWER POINT

68000  
68100  
68200  
68300  
68400  
68500

720

IC=IC+1  
IF(IC.EQ.7) IC=1  
NLNI=NLNT  
NLPI=NLPT  
NXOI=NXOT  
IF(IC.NE.IT) GO TO 700



EVALUATION OF OUTPUT PARAMETERS FOR 3 ADDITIONAL POINTS

68600  
68700  
68800  
68900  
69000  
69100  
69200  
69300  
69400  
69500

I3PTS=1  
JLNP=IEVAL(NLNT+1,NLPT,NXOT)  
JLNM=IEVAL(NLNT-1,NLPT,NXOT)  
JLPP=IEVAL(NLNT,NLPT+1,NXOT)  
JLPM=IEVAL(NLNT,NLPT-1,NXOT)  
JXOP=IEVAL(NLNT,NLPT,NXOT+1)  
JXOM=IEVAL(NLNT,NLPT,NXOT-1)

ICLN=-1  
IF(PMXPOWD(JLNP).GT.PMXPOWD(JLNM)) ICLN=1  
R1CLN=ICLN  
ICLP=-1  
IF(PMXPOWD(JLPP).GT.PMXPOWD(JLPM)) ICLP=1  
R1CLP=ICLP  
ICXD=-1  
IF(PMXPOWD(JXOP).GT.PMXPOWD(JXOM)) ICXD=1  
R1CXD=ICXD

69600  
69700  
69800  
69900  
70000  
70100  
70200  
70300  
70400  
70500

730

LNLP=IEVAL(NLNT+ICLN,NLPT+ICLP,NXOT)  
LNXD=IEVAL(NLNT+ICLN,NLPT,NXOT+ICXD)  
LPXD=IEVAL(NLNT,NLPT+ICLP,NXOT+ICXD)  
NLNI=NLNT+ICLN  
NLPI=NLPT+ICLP  
NXOI=NXOT  
IF(LNLP.EQ.0) GO TO 5  
IF(PMXPOWD(IET).LT.PMXPOWD(LNLP)) GO TO 710  
NLPI=NLPT  
NXOI=NXOT+ICXD  
IF(NXOI.EQ.NXOMIN) GO TO 732  
IF(LNXD.EQ.0) GO TO 5  
IF(PMXPOWD(IET).LT.PMXPOWD(LNXD)) GO TO 710  
NLNI=NLNT  
NLPI=NLPT+ICLP  
IF(LPXD.EQ.0) GO TO 5  
IF(PMXPOWD(IET).LT.PMXPOWD(LPXD)) GO TO 710

70600  
70700  
70800  
70900  
71000  
71100  
71200  
71300  
71400  
71500  
71600  
71700  
71800  
71900  
72000

EVALUATION OF COEFFICIENTS FOR POWER IN SECOND ORDER EXPANSION

72100  
72200  
72300

CALL COEFF(PMXPOWD)

72400  
72500

USE OF LIBRARY SUBROUTINE TO FIND INTERPOLATED MAXIMUM  
POWER POINT

72600  
72700  
72800

750

CALL SYMCO(AN,BM,XM,3,IDXXOM,1,ISS)  
IF(ISSU.NE.0) GO TO 750

72900  
73000



AM(2,1)=AM(1,1)=0  
AM(3,1)=AM(1,3)=0  
AM(2,3)=AM(3,2)=0  
CO TO 733

78530  
78540  
78550  
78560  
78700  
78800  
78900  
79000  
79100  
79200  
79300  
79400  
79500  
79550  
79500

FORMAT (1X,17HS)ACCESS FJLL EXIT , / )  
FORMAT (1X,5(2X,E13.6))  
FORMAT (1X)  
FORMAT (1X,9H MESHKNT =, I4, 9H LOOPKNT =, I4, / )  
FORMAT (/ , / , 1X, 9H MESHKNT =, I2, 1X, 9H PATHKNT =, I2, / )  
FORMAT (/ , / , 1X, 27H MAXIMUM EFFICIENCY VALUES , / , / )  
FORMAT (/ , / , 1X, 5H PIKNT, 6X, 7H CURDNET, 8X, 7H VOLTAGE, 8X, 3H ETA, / )  
FORMAT (1X,15,4(5X,E10.3))  
FORMAT (12X,E12.4)  
END

```

SUBROUTINE COEFF(DM)
COMMON IET, JLNP, JLNM, JLPP, JLPY, JXDP, JXDM, LNLP, LNXP, LPXD, RICLN,
RICLP, RICXC, BM(3,1), AM(3,3), JNLN(50), JNLP(50), JNXD(50), ID
DIMENSION DM(50)
AM(1,1)=(DM(JLNP)+DM(JLNM))/2.0-DM(IET)
BM(1,1)=(DM(JLNP)-DM(JLNM))/2.0
AM(2,2)=(DM(JLPP)+DM(JLPY))/2.0-DM(IET)
AM(2,1)=(DM(JLPP)-DM(JLPY))/2.0
AM(3,3)=(DM(JXDP)+DM(JXDM))/2.0-DM(IET)
BM(3,1)=(DM(JXDP)-DM(JXDM))/2.0
AM(1,2)=AM(2,1)=(DM(LNLP)-DM(IET)-BM(1,1)*RICLN-BM(2,1)*RICLP
-AM(1,1)-AM(2,2))/2.0/RICLN/RICLP
AM(1,3)=AM(3,1)=0.
AM(2,3)=AM(3,2)=0.
IF ((LNXC.EQ.0).OR.(LPXD.EQ.0)) RETURN
AM(1,3)=AM(3,1)=(DM(LNXP)-DM(IET)-BM(1,1)*RICLN-BM(3,1)*RICXC
-AM(1,1)-AM(3,3))/2.0/RICLN/RICXC
AM(2,3)=AM(3,2)=(DM(LPXD)-DM(IET)-BM(2,1)*RICLP-BM(3,1)*RICXC
-AM(2,2)-AM(3,3))/2.0/RICLP/RICXC
RETURN
END

```

79700  
79800  
79900  
80000  
80100  
80200  
80300  
80400  
80500  
80600  
80700  
80800  
80900  
81000  
81100  
81200  
81300  
81400

```
FUNCTION C(DIET, BM, AM, XM)  
DIMENSION AM(3, 3), BM(3, 1), XM(3, 1)  
D=DIET  
DO 800 I=1, 3  
D=D+BM(I, 1)*XM(I, 1)  
DO 800 J=1, 3  
D=D+AM(I, J)*XM(I, 1)*XM(J, 1)  
RETURN  
END
```

815.00  
817.00  
818.00  
819.00  
820.00  
821.00  
822.00  
823.00

,J)

```
FUNCTION IEVAL(NLNI,NLP1,NXO1)
COMMON IET, JLNP, JLNM, JLPP, JLPM, JXDP, JXDM, LNLP, LNXP, LPXP, RICLN,
IRICLP, RICXD, BM(3,1), AM(3,3), JNLN(50), JNLP(50), JNXO(50), ID
IP=0
IEVAL=0
810 IF(IP.EQ.ID) RETJRN
IP=IP+1
IF(NLNI.NE.JNLN(IP)) GO TO 810
IF(NLPI.NE.JNLP(IP)) GO TO 810
IF(NXO1.NE.JNXO(IP)) GO TO 810
IEVAL=IP
RETURN
END
```

824  
825  
826  
827  
828  
829  
830  
831  
832  
833  
834  
835  
836

```

ROUTINE CRVFIT(CRNT,VOLT,PTKNT,INDEXTA,CURDNET,PMAXPOW) 83700
POWER,PTKNT 83800
DIMENSION VOLT(30),CRNT(30),CM(30,30),T(30),TIM1(30),POWER(30) 83900
INDEXTA(30) 84000

POWER IN TERMS OF CURRENT AND VOLTAGE 84100
84200
DO 1 I=1,PTKNT 84300
POWER(I)=VOLT(I)*CRNT(I) 84400
84500
84600
FIND POLYNOMIAL EXPRESSION FOR POWER IN TERMS OF SKEWED CURRENTS 84700
84800
K1=AMAX1(CRNT(PTKNT),CRNT(PTKNT-1),CRNT(PTKNT-2)) 84900
K2=AMAX1(POWER(PTKNT),POWER(PTKNT-1)) 85000
DO 2 I=1,PTKNT 85100
M(I,1)=1 85200
M(I,2)=CRNT(I)-SKEW*POWER(I) 85300
DO 3 J=2,PTKNT 85400
M(I,J)=CM(I,J-1)*CRNT(I) 85500
CALL LINEQ1(CM,POWER,T,30,PTKNT,1,ILE) 85600
WRITE(5,3) ILE 85700
FORMAT(5HILE = ,11) 85800
85900
86000
FIND THE MAXIMUM POWER POINT 86100
86200
DO 4 I=2,PTKNT 86300
TIM1 I=1 86400
TIM1(I)=I(I)*R1M) 86500
CRNT1=CRNT(I) 86600
CRNT2=CRNT(PTKNT-I) 86700
DO 5 J=1,3 86800
PP1=POWER(PTKNT,I,TIM1,CRNT1) 86900
PP2=POWER(PTKNT,I,TIM1,CRNT2) 87000
PP=(PP1+PP2)/2 87100
CRNT1=(PP1*CRNT2+PP2*CRNT1)/(PP1+PP2) 87200
CRNT2=CRNT1 87300
CRNT=CURDNET 87400
CONTINUE 87500

COMPUTATION OF MAXIMUM POWER 87600
87700
PPMAXPOW=0. 87800
DO 7 J=1,PTKNT 87900
PPMAXPOW=PPMAXPOW+I(I)*CRNT1 88000
CRNT1=CRNT1+CRNT(I) 88100
88200
SKEW CURRENT AT MAXIMUM POWER POINT 88300
88400
POWER=CURDNET*SKEW*PPMAXPOW 88500
WRITE(5,4) 88600
88700
88800

```



DIMENSION TIME(30)  
 TIME=0.  
 I=1, PTKNF  
 TIME=PPRIME+TIME(I)\*CTM2  
 TIME=CCINZ+CCJRDNET  
 PTKNF  
 PTKNF

8870  
 8900  
 8910  
 8920  
 8930  
 8940  
 8950  
 8960  
 8970  
 8980

1.0644E1

0.3113E19

3.4637E19

1.0000E-03	3.7778E+19	2.6068E+21
1.1000E-03	4.0326E+19	1.6745E+21
1.2000E-03	4.2154E+19	1.2834E+21
1.3000E-03	4.3592E+19	1.0335E+21
1.4000E-03	4.4770E+19	8.6096E+20
1.5000E-03	4.5764E+19	7.3683E+20
1.6000E-03	4.6625E+19	6.4419E+20
1.7000E-03	4.7384E+19	5.7268E+20
1.8000E-03	4.8053E+19	5.1579E+20
1.9000E-03	4.8678E+19	4.6935E+20
2.0000E-03	4.9239E+19	4.3059E+20
2.1000E-03	4.9756E+19	3.9764E+20
2.2000E-03	5.0235E+19	3.6921E+20
2.3000E-03	5.0681E+19	3.4438E+20
2.4000E-03	5.1107E+19	3.2247E+20
2.5000E-03	5.1488E+19	3.0296E+20
2.6000E-03	5.1856E+19	2.8547E+20
2.7000E-03	5.2202E+19	2.6970E+20
2.8000E-03	5.2531E+19	2.5540E+20
2.9000E-03	5.2842E+19	2.4237E+20
3.0000E-03	5.3137E+19	2.3046E+20
3.1000E-03	5.3418E+19	2.1952E+20
3.2000E-03	5.3686E+19	2.0945E+20
3.3000E-03	5.3942E+19	2.0016E+20
3.4000E-03	5.4187E+19	1.9155E+20
3.5000E-03	5.4421E+19	1.8356E+20
3.6000E-03	5.4646E+19	1.7619E+20
3.7000E-03	5.4862E+19	1.6919E+20
3.8000E-03	5.5069E+19	1.6272E+20
3.9000E-03	5.5269E+19	1.5666E+20
4.0000E-03	5.5461E+19	1.5097E+20
4.1000E-03	5.5646E+19	1.4564E+20
4.2000E-03	5.5825E+19	1.4061E+20
4.3000E-03	5.5998E+19	1.3588E+20
4.4000E-03	5.6165E+19	1.3142E+20
4.5000E-03	5.6327E+19	1.2720E+20
4.6000E-03	5.6483E+19	1.2321E+20
4.7000E-03	5.6635E+19	1.1943E+20
4.8000E-03	5.6782E+19	1.1585E+20
4.9000E-03	5.6924E+19	1.1244E+20
5.0000E-03	5.7063E+19	1.0921E+20
5.1000E-03	5.7197E+19	1.0613E+20
5.2000E-03	5.7328E+19	1.0320E+20
5.3000E-03	5.7456E+19	1.0040E+20
5.4000E-03	5.7579E+19	9.7730E+19
5.5000E-03	5.7701E+19	9.5182E+19
5.6000E-03	5.7817E+19	9.2745E+19
5.7000E-03	5.7932E+19	9.0413E+19
5.8000E-03	5.8043E+19	8.8180E+19
5.9000E-03	5.8152E+19	8.6040E+19
6.0000E-03	5.8258E+19	8.3988E+19
6.1000E-03	5.8362E+19	8.2018E+19
6.2000E-03	5.8464E+19	8.0123E+19
6.3000E-03	5.8563E+19	7.8300E+19
6.4000E-03	5.8659E+19	7.6550E+19
6.5000E-03	5.8754E+19	7.4870E+19

7.2500E-02	5.8937E+19	7.1693E+19
7.3750E-02	5.9026E+19	7.0188E+19
7.5000E-02	5.9113E+19	6.8735E+19
7.6250E-02	5.9198E+19	6.7334E+19
7.7500E-02	5.9281E+19	6.5980E+19
7.8750E-02	5.9363E+19	6.4673E+19
8.0000E-02	5.9443E+19	6.3408E+19
8.1250E-02	5.9521E+19	6.2186E+19
8.2500E-02	5.9598E+19	6.1003E+19
8.3750E-02	5.9674E+19	5.9858E+19
8.5000E-02	5.9748E+19	5.8749E+19
8.6250E-02	5.9821E+19	5.7675E+19
8.7500E-02	5.9892E+19	5.6633E+19
8.8750E-02	5.9962E+19	5.5623E+19
9.0000E-02	6.0031E+19	5.4644E+19
9.1250E-02	6.0099E+19	5.3693E+19
9.2500E-02	6.0165E+19	5.2770E+19
9.3750E-02	6.0231E+19	5.1874E+19
9.5000E-02	6.0295E+19	5.1004E+19
9.6250E-02	6.0358E+19	5.0157E+19
9.7500E-02	6.0420E+19	4.9335E+19
9.8750E-02	6.0482E+19	4.8535E+19
1.0000E-01	6.0542E+19	4.7757E+19